Ultrasonics Sonochemistry 100 (2023) 106617

Contents lists available at ScienceDirect

Ultrasonics Sonochemistry

journal homepage: www.elsevier.com/locate/ultson

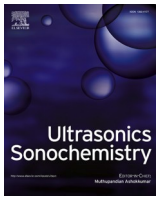

Sonodynamic therapy-based nanoplatforms for combating bacterial infections

Pei-Yao Xu [a,b], Ranjith Kumar Kankala [a,b], Shi-Bin Wang [a,b], Ai-Zheng Chen [a,b,*]

[a] Institute of Biomaterials and Tissue Engineering, Huaqiao University, Xiamen, Fujian 361021, PR China
[b] Fujian Provincial Key Laboratory of Biochemical Technology, Huaqiao University, Xiamen, Fujian 361021, PR China

ARTICLE INFO

Keywords:
Antibacterial
Antibiofilm, Sonodynamic Therapy
Bacterial infection
Nanoplatform

ABSTRACT

The rapid spread and uncontrollable evolution of antibiotic-resistant bacteria have already become urgent global to treat bacterial infections. Sonodynamic therapy (SDT), a noninvasive and effective therapeutic strategy, has broadened the way toward dealing with antibiotic-resistant bacteria and biofilms, which base on ultrasound (US) with sonosensitizer. Sonosensitizer, based on small organic molecules or inorganic nanoparticles, is essential to the SDT process. Thus, it is meaningful to design a sonosensitizer-loaded nanoplatform and synthesize the nanoplatform with an efficient SDT effect. In this review, we initially summarize the probable SDT-based antibacterial mechanisms and systematically discuss the current advancement in different SDT-based nanoplatform (including nanoplatform for organic small-molecule sonosensitizer delivery and nanoplatform as sonosensitizer) for bacterial infection therapy. In addition, the biomedical applications of SDT-involved multifunctional nanoplatforms are also discussed. We believe the innovative SDT-based nanoplatforms would become a highly efficient next-generation noninvasive therapeutic tool for combating bacterial infection.

1. Introduction

Uncontrollable harmful bacterial infection has posed an enormous threat to public health and the economy for centuries [1]. Although the traditional antibiotic therapy has a positive effect in killing the bacteria, the poor therapeutic efficiency due to the generation of antibiotics-resistant pathogens fails the eliminate the pathogens in the clinic [2]. With the evolution of bacteria, drug-resistant bacteria could produce related enzymes to restrict the antibiotics from entering cells, alter the membrane barrier and permeability, or develop drug efflux pumps protecting themselves from the antibacterial agents [3]. More importantly, over 80 % of bacterial infections are related to biofilm, composed of extracellular polymeric substances (EPS) coated aggregates of bacteria [4]. The dense structural and functional heterogeneity of biofilm can protect pathogens from host immune response, inhibit drug penetration and restrain antibiotics by enzymatic degradation or adsorption [5,6]. Developing powerful antibacterial strategies and antibiofilm therapeutics without drug tolerance is a crucial challenge that needs to be conquered in the scientific community.

Recently, some antibiotics-free and non-invasive approaches have been developed, such as light-medicated photodynamic therapy (PDT) and photothermal therapy (PTT), and ultrasound (US)-triggered sonodynamic therapy (SDT) [7–9]. Among these approaches, SDT is the most promising bacterial infection modality due to its excellent tissue-penetrating activity and effectiveness against drug-resistant bacteria, even biofilm [10]. Moreover, US-triggered local SDT treatment has been applied as a minimally-invasive tool to replace antibiotic therapy, which could avoid the potential systemic toxicity and reduce bacterial resistance that troubled conventional antibiotic therapy [11]. In the US-based therapy process, sonosensitizer is the most essential factor [12]. Although small-molecule of sonosensitizer have been exploited for damaging pathogenic bacteria, their clinical applications are still limited by the potential toxicity and unsatisfied stability [13].

The rapid development of nanoparticles for drug loading and delivery has achieved sustainable innovation in medicine [14–16]. Owing to the superior properties, those nanocarriers could enhance the pharmacokinetic profile *in vivo* and the therapeutic effect of small-molecule sonosensitizers [17]. More importantly, inorganic nanoparticles such as titanium dioxide (TiO_2) and barium titanate (BTO) could directly act as sonosensitizers due to their intrinsic sonosensitivity properties [18,19]. Moreover, the nanostructures of those organic sonosensitizers not only provided more nucleation sites for reactive oxygen species (ROS)

* Corresponding author.
E-mail address: azchen@hqu.edu.cn (A.-Z. Chen).

https://doi.org/10.1016/j.ultsonch.2023.106617
Received 26 May 2023; Received in revised form 20 September 2023; Accepted 22 September 2023
Available online 23 September 2023

generation, but also exhibited better stability in SDT application [20].

Herein, we focus on the recent achievements of nanoplatform for the delivery of sonosensitizer and US-triggered nanoplatform with antibacterial properties (Fig. 1). The current medical application of SDT antibacterial strategies, such as skin infection, osteomyelitis, implant infection, myositis, periodontal infection, lung infection, *Helicobacter pylori (H. pylori)* infection, etc., are systematically reviewed. Moreover, we provided a brief perspective on the continuing challenges as well as future research directions in SDT-involved antibacterial strategies.

2. SDT antibacterial mechanism

2.1. Ros-dependent damage

US-triggered ROS production is the main reason for SDT-based bacterial killing and biofilm elimination. Although the mechanism of US-triggered ROS generation is unclear, the cavitation effect and sonoluminescence effect are two fundamental assumptions to explain the reason for the sonosensitizer-mediated ROS generation under US treatment [21]. The ultrasonic cavitation effect is an instantaneous physical phenomenon that happens in liquid promoted by sonosensitizers with US irradiation, which could be divided into the microbubble formation and expansion process and the microbubble broken process [22]. Notably, the generated energy was released into heat (>10000 K) and pressure (>81 MPa), to induce the pyrolysis reaction of water or sonosensitizers, which would generate ROS, such as hydroxyl radicals (•OH), singlet oxygen ($^1O_2$), and superoxide anion ($O_2^{\bullet-}$) [23–25]. In addition, the collapsing of gas bubbles could cause sonoluminescence, which excited the electron orbitals of sonosensitizer for electron-hole production and generated ROS subsequently [26,27]. The generated ROS could elicit bacterial damage by reacting with various biomacromolecules, inducing protein denaturation, resulting in lipid oxidative degradation, and damaging DNA [28].

2.2. Mechanical and thermal damage

SDT induced sonomechanical damage is an important antibacterial mechanism that acts on bacteria by destroying the cell membrane. As mentioned above, the interaction between US and sonosensitizer could lead the cavitation effect, which may induce some mechanical effects, including liquid microjets, microstreaming shock waves, and shear force [22]. These effects that induced by the interaction between the sonosensitizer and US could cause pore formation in cell membranes, disrupting bacterial cells and improving the drug permeability [29]. Moreover, the microjets generated during bubble collapse, shock waves formed on the destruction of an inertial bubble, and microstreaming could also inhibit the biofilm formation process and destroy the biofilm from the material surface [30].

In addition, the energy absorption and transformation induced by ultrasonic cavitation can lead to the rising temperature of the surrounding environment. The hyperthermia effects could be controlled by different US conditions such as US intensity, duty cycle, and duration, which might damage the cytoskeleton and destroy bacterial biomolecules in bacterial cells [31].

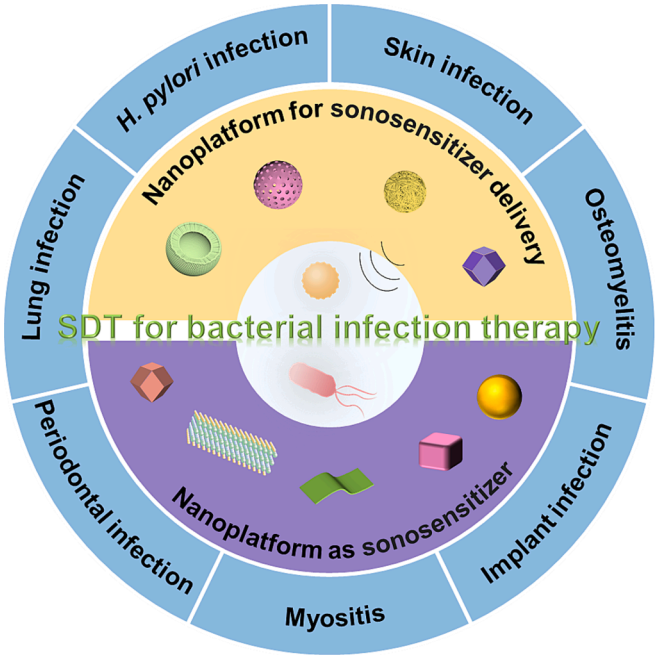

Fig. 1. Overall classification and overview of nanoplatforms-based SDT for bacterial infection therapy.

3. Nanoplatform for delivery of organic small-molecule sonosensitizer

Sonosensitizer is a fundamental prerequisite in antibacterial SDT, resulting in a chain of reactions under US activation to stimulate bacterial death [32]. Small molecules of organic photosensitizers, such as porphyrin derivatives [33], chlorin e 6 (Ce6) [34], indocyanine green (ICG) [35,36], and curcumin [37], have exhibited potent ROS generation activity with US treatment. Due to the poor solubility, potential phototoxicity, and short blood circulation time of most organic small-molecule reported sonosensitizers, the SDT therapeutic effects of those sonosensitizers were limited applicability in clinics. Owing to the high-quality development of nanomedicine, different drug-carrier nanoplatforms, including liposome nanocarriers, polymer nanoparticles, inorganic nanoplatforms, and organic/inorganic hybrid nano-carriers have been developed to deliver organic small-molecule sonosensitizers for SDT application [31,38,39]. Those nanoplatforms have enhanced the bioavailability and the SDT efficacy of organic small-molecule sonosensitizers against various pathogens. Regarding sonosensitizers delivery carriers, they could be divided into three types (Table 1): Organic carrier, inorganic carrier, and organics/inorganics hybrid carrier.

3.1. Delivery of organic small-molecule sonosensitizer with organic carriers

3.1.1. Liposomes

Liposomes possess outstanding features, including high biocompatibility, easy functionalization, and fabrication, and have been extensively used in sonosensitizers encapsulation for antibacterial treatment [40]. The unusual core–shell microstructure of liposome is suitable for delivering hydrophilic and hydrophobic drugs [41]. For example, Maryam et al. loaded emodin into nanoliposomes (N-EMO) based on cholesterol and lecithin for SDT-induced anti-biofilm effects [42]. N-EMO inhibited the *Pseudomonas aeruginosa* (*P. aeruginosa*), *Staphylococcus aureus* (*S. aureus*), and *Acinetobacter baumannii* (*A. baumannii*) biofilm growth with SDT treatment by downregulating the genes (*lasI*, *agrA*, and *abaI*) expression levels. In addition to bioavailability improvement, researchers have synthesized a series of multifunctional liposome nanoparticles for monitoring infectious sites and precise elimination of bacteria. Wang et al. constructed an ICG-loaded monoclonal antibody-conjugated nanoliposome (HpAb-LiP-ICG) using the thin film dispersion method against *H. pylori* based on SDT [43]. Similarly, Pang et al. designed a nanoliposome based on maltohexaose-modified cholesterol and bacteria-targeted lipid for purpurin 18 (MLP18) delivery [44]. This bacteria-activated nanoplatform allowed accurate discrimination between bacterial infected tissue, cancer site or inflammation site without bacteria, and finally exhibited an improvement in antibacterial performance by P18-mediated SDT. This outstanding bacteria-targeting activity produced significant benefits for

Table 1
A summary of nanoplatform for antibacterial SDT for the delivery of organic small-molecule sonosensitizer.

Category	Name	Microorganism	Organic small-molecule sonosensitizers	US conditions	Reference
Organic carriers	N-EMO	*S. aureus, P. aeruginosa,* and *A. baumannii*	emodin	1.0 MHz, 2.0 W /cm^2, 5 min	[42]
	Hp Ab-LiP-ICG	*H. pylori*	ICG	1.0 MHz, 1.5 W /cm^2, 10 min	[43]
	MLP18	MRSA	purpurin 18	1.0 MHz, 0.97 W/cm^2, 5 min	[44]
	CUR/TSIIA/CS	*S. aureus*	curcumin	1.0 MHz, 3.0 W/ cm^2, 10 min	[47]
	MB-loaded PLGA	*P. gingivalis*	MB	1.0 MHz; 1.56 W/cm^2, 1 min	[48]
	M2/IR780@PLGA	MRSA	IR780	1.0 MHz, 50 % duty cycle, 2.0 W/ cm^2, 4 min	[49]
	NM@Cur	*S. mutans*	curcumin	1.56 W/cm^2, 1 min	[50]
	PPPC-1	*S. aureus* and MRSA	MnTCPP	1.0 MHz, 1.5 W/cm^2, 9 min	[51]
	IR780@PLGA	MRSA	IR780	1.0 MHz, 2.0 W/cm^2, 3.5 min	[62]
Inorganic carriers	M@P-Fe	*S. aureus*, *S. mutans*, and *E. faecalis*	PpIX	1.0 MHz, 0.5 W/cm^2, 3 min	[54]
	UCNP@mSiO_2(RB)-Ag	MRSA	rose bengal	2.0 W/cm^2, 10 min	[55]
	CuS/Cur	*S. aureus*	curcumin	1.0 MHz, 50 % duty cycle, 1.0 W/ cm^2, 15 min	[56]
Organic/inorganic hybrid carriers	SPI	MRSA and *E. coli*	ICG	–	[57]
	MAPC	MRSA	Ce6	1.0 MHz, 1.0 W/cm^2, 10 min	[58]
	TPPS@Au	MRSA	TPPS	2.85 MHz, 10 Vp-p, 5 min	[59]
	HFH@ZIF-8	MRSA	HMME	0.5 MHz, 50 % duty cycle, 1.2 W/ cm^2, 10 min	[60]
	HMMP	*S. aureus*	PpIX	0.04 MHz, 1 min per cycle, 1.5 W/ cm^2, 5 min	[61]
	Pd@Pt-T790	MRSA	T790	1.0 MHz, 50 % duty cycle, 0.97 W/ cm^2, 8 min	[63]

bacterial clearance based on SDT.

3.1.2. Polymer nanoparticles

Polymer-based nanocomposites have shown a superior capability for enhancing the delivery of sonosensitizer by improving the stability and protecting them from the elimination of the body [45]. In particular, the lower toxicity and inflammatory reactions of polymer meet the demand for sonosensitizers delivery for clinical translation [46].

Natural polymers are promising in SDT-based processes due to their bioactivity and biocompatibility. Su et al. proposed chitosan (a natural antibacterial polymer) nanocomposite by antisolvent precipitation method for loading curcumin and Tanshinone IIA (CUR/TSIIA/CS) [47]. The size reduction enhanced the equilibrium solubility of both drugs in distilled water, which also showed a sustained drug release activity for 6 days. Under US irradiation, curcumin in CUR/TSIIA/CS effectively generated ROS for destroying bacteria. Moreover, the inhibition of immune responses by Tanshinone IIA was further enhanced after combination with anti-inflammatory and antibacterial effects, which had achieved excellent therapeutic outcomes in *S. aureus*-infected otitis media model *in vivo*.

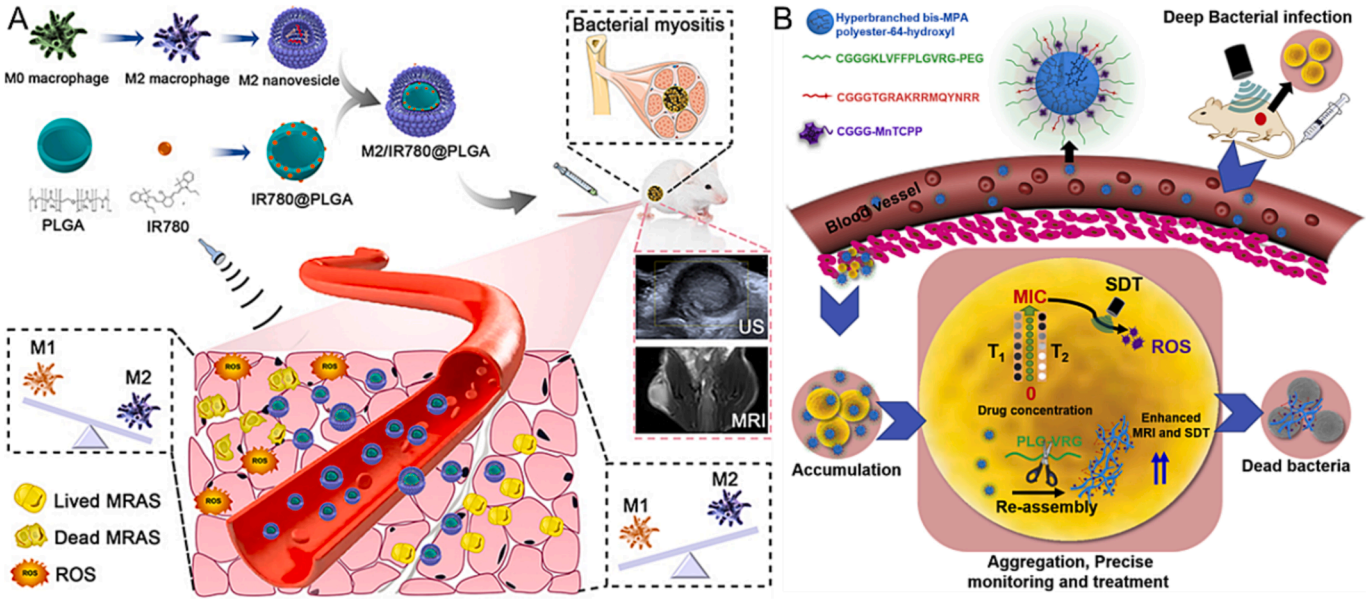

Fig. 2. (A) Schematic illustration of the M2/IR780@PLGA nanoparticles for antibacterial SDT. Reproduced with permission [49]. (B) Schematic illustration of enzyme-induced morphology transformation of PPPC for precise MRI-guided treatment of drug-resistant bacterial deep infection. Reproduced with permission [51].

Synthetic polymers offer obvious advantages, including clear chemical structure, mature synthetic routes, and mass production with stable quality. A biodegradable copolymer poly (lactic-co-glycolic acid) (PLGA) is an ideal candidate for delivery sonosensitizer. Aldegheishem et al. synthesized methylene blue (MB)-loaded PLGA nanoparticles for photo-sonodynamic therapy, exhibiting excellent antibacterial effect against *Porphyromonas gingivalis* (*P. gingivalis*) without causing any surface damage of implant [48]. Similarly, Chen et al. constructed a novel PLGA-based nanoplatform named M2/IR780@PLGA, which was constructed with IR780-loaded PLGA nanoparticles that coated with M2 macrophages cell membranes (Fig. 2**A**) [49]. The obtained M2/IR780@PLGA not only realized the US-triggered SDT effect for bacterial-killing but also accumulated at the inflammation site.

Maryam et al. developed a polyethylene glycol-l-α phosphatidyl ethanolamine-based nanomicelles (NM@Cur) for curcumin loading, which showed higher stability and *Streptococcus mutans* (*S. mutans*) killing activity [50]. The NM@Cur greatly enhanced the ROS level in cells under US treatment and achieved antibacterial efficiency of 99.9 % at concentrations of 50 mM. Besides, the real-time monitoring of infection sites plays a crucial role in the antibacterial process. Wang et al. fabricated a transformable polymer-peptide-porphyrin conjugate (PPPC) loaded porphyrin sonosensitizer (MnTCPP) nanoplatform (PPPC-1) for magnetic resonance imaging (MRI)-guided SDT (Fig. 2**B**) [51]. After intravenous injection, the polyethylene glycol (PEG) shell of PPPC-1 was broken up by gelatinase-cleavable peptide, resulting in the formation of nanoaggregates based on the hydrophilic-hydrophobic interactions. The above process facilitated the drug accumulation in bacterial deep infection sites, resulting in higher SDT-based antibacterial effects compared with morphology-unchanging nanoplatform.

3.2. Delivery of organic small-molecule sonosensitizer with inorganic carriers

Considering their superior physicochemical properties, high stability, sufficiently high surface area, and simplicity of fabrication, inorganic carriers are generally used as excellent carriers for sonosensitizers encapsulation [52]. Among the heterogeneous types of inorganic nanoparticle family, mesoporous silica nanoplatform (MSN) was an excellent option for loading sonosensitizer due to their adjustable microstructure (such as shape, morphology, pore size) and ease of surface functionalization [53]. In recently work, Guo et al. developed a novel nanoplatform (M@P-Fe) based on MSN nanoparticles by conjugating with protoporphyrin IX (PpIX) and functionalizing with iron ions [54]. The M@P-Fe possessed loading efficiency of PpIX (3.6 %) and iron content at 1.03 %, displaying a higher *Enterococcus faecalis* (*E. faecalis*) killing effect induced by Fenton-enhanced SDT. M@P-Fe achieved comparable antibacterial and anti-biofilm effects to commercial sodium hypochlorite (NaClO) irrigant under US irradiation and displayed lower toxicity to mouse osteoblastic (MC3T3-E1) cells. Zhao et al. prepared a core–shell structured nanoplatform for loading rose bengal and silver nanoparticles (UCNP@mSiO_2(RB)-Ag), constructed by the MSN as shell and up-conversion nanoparticle as core [55]. Upon 980 nm laser irradiation and US irradiation, UCNP@mSiO_2(RB)-Ag induced excellent $^1O_2$ production and sustained by Ag^+ release inhibition activity, demonstrating high synergistic antibacterial efficacy of SDT-PDT strategy.

In addition to traditional MSN, copper sulfide (CuS) nanoparticles with PTT or PDT effect have been demonstrated as novel nanoplatforms for delivery sonosensitizers. For example, Liu et al. loaded curcumin on petaloid CuS nanoparticles through in situ nucleation and growth to construct CuS/Cur hybrid nanoplatform [56]. Triggered by US and near-infrared vibration, the produced electrons for Cur gathered on CuS, resulting in the electron transfer acceleration, subsequently promoting the ROS generation. Remarkably, after the combined treatment based on the high temperature, ROS, and drug characteristics, CuS/Cur inhibited *S. aureus* growth with good cytocompatibility.

3.3. Delivery of organic small-molecule sonosensitizer with organics/inorganics hybrid carriers

Organic/inorganic hybrid carriers assimilated the advanced advantages of organic and inorganic compositions, which possessed versatile functions, got an extensive application in organic small-molecule sonosensitizers encapsulation, and produced synergistic effects for SDT-based antibacterial strategy. Recently, Huang et al. synthesized a polyethyleneimine (PEI) coated selenium nanoparticles-based nanoplatform to achieve ICG loading (SPI), achieving significant *Escherichia coli* (*E. coli*) killing activity under US and visible light stimulation [57]. Dong et al. synthesized PEG-coated manganese dioxide nanosheets for loading Ce6 and α-amylase (MAPC) [58]. MAPC exhibited the efficient extracellular substances of biofilms ability and catalyzed the hydrogen peroxide (H_2O_2) into oxygen (O_2), which significantly generated ROS with US irradiation in infected tissue. The fluorescence imaging of infected mice indicated that the MAPC with pH-responsive Ce6-releasing properties showed an excellent antibacterial effect upon additional US treatment. Another study took the advantages of Au and organic sonosensitizers, Sun et al. developed by Au nanorod coated thiol-poly (N, N-diethylacrylamide) for *meso*-tetrakis(4-sulfonatophenyl) porphyrin (TPPS@Au) loading [59]. TPPS@Au presented SDT antibacterial performance and performed multimodal motion via US propulsion.

In addition to modifying inorganic nananostructures with polymers to enhance their bioactivity and biocompatibility, functional biomacromolecules were utilized to create hybrid nanostructures for SDT-based antibacterial enhancement. As to conquer the difficulties of insufficient O_2 in the SDT process, Geng et al. reported O_2-carrying component nanostructures (HFH@ZIF-8), based on zeolitic imidazolate framework-8 loaded with hematoporphyrin monomethyl ether (HMME), and then modified with hemoglobin [60]. HFH@ZIF-8 offered sufficient O_2 in the SDT process, which displayed higher ROS generation efficiency. After intravenous tail-vein injection, HFH@ZIF-8 nanocomposites were proved to target the inflammation site efficiently in methicillin-resistant *S. aureus* (MRSA) caused myositis and accelerate infection disease recovery after US stimulation. A combination of cell membrane-targeted strategies was also used to improve the SDT effect. Lin et al. presented a hybrid nanovesicle for the sono-immunotherapy of bacterial infection, which was established by the PpIX-loaded hollow manganese oxide (MnO) coated by hybrid membrane vesicles integrating with mouse breast carcinoma cell (4T1) and mouse macrophage (RAW264.7) (HMMP) [61]. With the modification of RAW264.7 membranes, the HMMP accumulated at the infectious microenvironment and produced O_2 for ROS generation-based PpIX-induced SDT antibacterial strategy. Furthermore, combining 4T1 membrane antigens and manganese ions recruited and promoted the immune-related cells. Together, the combination of nano vaccine and US stimulation triggered local antibacterial immune responses, which also induced systemic immunological responses for long-term protection from bacteria invasion.

4. Nanoplatform as sonosensitizer

Although nanodrug carrier system significantly enhanced the SDT effects of organic small-molecule sonosensitizer, the lower loading efficacy and the inevitable leakage of the entrapped organic sonosensitizer are still existing. Compared with traditional organic small-molecule sonosensitizer, nano-sonosensitizer with outstanding stability and physicochemical properties, which could act as a powerful tool based on SDT effect in bacterial killing and biofilm elimination application. This section reviews different classes of nano-sonosensitizers and discusses their related progresses for antibacterial application (Table 2).

4.1. Titanium-based nanoplatforms

Titanium-based nanoplatform (e.g., TiO_2, titanate, titanium

Table 2
Examples of nano-sonosensitizers for antibacterial SDT.

Type	Material	Microorganism	US conditions	Reference
TiO_2-based nanoplatforms	anatase-brookite TiO_2	*S. aureus*	1.0 MHz, 50 % duty cycle, 1.5 W/cm^2, 15 min	[68]
	TiOx nanofibers dotted with $Ti_2C(OH)_2$ nanosheets	*E. coli*	1.0 MHz, 50 % duty cycle, 1.0 W/cm^2, 4 min	[69]
	Ti-S-TiO_{2-x}	*S. aureus*	1.0 MHz, 50 % duty cycle, 1.5 W/cm^2, 15 min	[71]
	CuO_2/TiO_2	MRSA	1.0 MHz, 1.0 W/cm^2, 5 min	[72]
	Au NPs-TNTs	*P. gingivalis*	1.0 MHz, 1.5 W/cm^2, 20 min	[73]
	mTiO_2@PDA	*E. coli* and *S. aureus*	3.0 MHz, 1.5 W/cm^2, 5 min	[74]
	DT-Ag-CS^+	*P. gingivalis*	1.0 MHz, 50 % duty cycle, 1.0 W/cm^2, 5 min	[112]
	Au/TNT@PG	MRSA	1.0 MHz, 50 % duty cycle, 1.5 W/cm^2, 8 min	[113]
BTO-based nanoplatforms	BT-OHA/THM-APMH	*E. coli* and *S. aureus*	1.0 MHz, 1.5 W/cm^2,10 min	[76]
	BTO@ZIF-8/CIP	*S. aureus*	1.0 MHz, 50 % duty cycle, 1.5 W/cm^2, 5 min	[77]
	Vo-BTO	*E. coli* and *S. aureus*	0.75 W/cm^2, 4 min	[78]
	SDBTO	*S. aureus*	1.0 MHz, 50 % duty cycle, 0.5 W/cm^2, 5 min	[79]
	Au@BTO	*E. coli* and *S. aureus*	1.0 MHz, 50 % duty cycle, 1.5 W/cm^2, 3 min	[80]
	Ag NWs@$BaTiO_3$	*E. coli* and *S. aureus*	80 W, 2 L	[114]
Mo-based nanoplatforms	MoS_2 nanosheets	*S. aureus* and *P. aeruginosa*	1.0 MHz, 50 % duty cycle, 1.5 W/cm^2, 3 min	[82]
	g-ZnN_4-MoS_2	MRSA	1.0 MHz, 50 % duty cycle, 1.5 W/cm^2, 20 min	[83]
	$MoSe_2$ NF	MRSA	1.0 MHz, 0.3 W/cm^2, 5 min	[84]
	SMB NPs	*S. aureus*	1.0 MHz, 50 % duty cycle, 0.5 W/cm^2, 5 min	[85]
	MoO_x@Mo_2C	MRSA	1.0 MHz, 50 % duty cycle, 1.0 W/cm^2, 5 min	[86]
	MoS_2/Cu_2O	*S. aureus*	1.0 MHz, 1.5 W/cm^2, 20 min	[115]
Carbon-based nanoplatforms	NM-Ti_3C_2-SD(Ti^{3+})	MRSA	1.0 MHz, 50 % duty cycle, 1.0 W/cm^2, 10 min	[91]
	LS-Ti_3C_2	MRSA	1.0 MHz, 50 % duty cycle, 1.0 W/cm^2, 20 min	[90]
	$BiFeO_3/Ti_3C_2$	*S. aureus*	1.0 MHz, 2.5 W/cm^2, 20 min	[93]
	ZnO@GDY NR	MRSA and *P. aeruginosa*	1.0 MHz, 50 % duty cycle, 1.0 W/cm^2, 30 min	[94]
	PtRu/C_3N_5	MRSA, *S. aureus, E. coli,* and *P. aeruginosa*	1.0 MHz, 1.0 W/cm^2, 10 min	[95]
	CaO_2-TiOx@Ti_3C_2	MRSA	1.0 MHz, 50 % duty cycle, 1.0 W/cm^2, 5 min	[92]
Noble metals-based nanoplatforms	Ag_2O_2	MRSA, *S. aureus, E. coli,* and *P. aeruginosa*	1.0 MHz, 1.0 W/cm^2, 10 min	[97]
	PtCu	*E. coli* and *S. aureus*	0.04 kHz, 3.0 W/cm^2, 8 min	[98]
	Au@Cu_2O	*S. aureus*	1.0 MHz, 50 % duty cycle, 1.5 W/cm^2, 15 min	[99]
	SnSNs@hydrogel	MRSA	1.5 W/cm^2, 5 min	[100]
	CuO_2-BSO@Gel	*E. coli* and *S. aureus*	1.0 MHz, 50 % duty cycle, 1.5 W/cm^2, 4 min	[101]
	Cu_2MoS_4	MRSA	1.0 MHz, 50 % duty cycle, 1.0 W/cm^2, 5 min	[116]
MOF-based nanoplatforms	D-PCN-2	MRSA	1.0 MHz, 50 % duty cycle, 1.5 W/cm^2, 20 min	[105]
	MIL@Ag-PEG	*S. aureus*	2.0 W/cm^2, 15 min	[106]
	CeTCPP-Au	*E. coli* and *S. aureus*	1.0 MHz, 50 % duty cycle, 1.7 W/cm^2, 20 min	[107]
	MOF@Au-DNase I	*S. aureus*	1.5 W/cm^2, 10 min	[108]
	HNTM/Nb_2C	MRSA	1.0 MHz, 50 % duty cycle, 1.5 W/cm^2, 15 min	[109]
	RBC-HNTM-MoS_2	MRSA	1.0 MHz, 50 % duty cycle, 1.5 W/cm^2, 15 min	[110]
	HN-Ti_3C_2	MRSA	1.0 MHz, 50 % duty cycle, 1.5 W/cm^2, 15 min	[117]
	HMME@DHA@MPN	*H. pylori*	1.0 MHz, 70 % duty cycle, 1.5 W/cm^2, 6 min	[118]

carbides) have now attracted considerable researchers' interest, owing to their tunable structure and their special physicochemical properties, high chemical stability, and excellent ROS generation ability during ultrasonic irradiation, lower phototoxicity than organic sonosensitizers [64–67]. Numerous titanium-based nano-sonosensitizers have been designed and applied in antibacterial and antibiofilm therapy based on SDT. For instance, Ou-yang et al. fabricated TiO_2 with different phases, including anatase, rutile, anatase–rutile, anatase-brookite, and anatase-brookite-rutile [68]. The results showed that TiO_2 with anatase-brookite phases exhibited lower electron-hole recombination efficiency and better ROS generation performance upon US irradiation. Zhu et al. constructed a novel sticking-bacteria gel based on $Ti_2C(OH)_2$ nanosheets dotted amorphous TiOx nanofibers, which efficiently restrained bacteria invasions by binding with bacteria [69]. According to the 1,3-diphenylisobenzofuran (DPBF) results with US treatment, the nanocomposite had a more substantial ROS generation effect than TiO_2 NPs. Moreover, $Ti_2C(OH)_2$ with a catalase-like activity provided enough O_2 in the infection site for promoted SDT against bacteria, showing this nanocomposite could use as a SDT antibacterial agent for killing bacteria and wound healing promotion.

To improve the quantum yield SDT effect of TiO_2-based sonosensitizers, doping other elements on TiO_2 can significantly increase ROS production rate or achieve synergistic antibacterial activity [70]. For instance, Su et al. modified the surface of the Ti implant with oxygen-deficient sulfur-doped TiO_2 (Ti-S-TiO_{2-x}), which was utilized in bone implant infection elimination through synergistic PTT/SDT (Fig. 3**A**) [71]. Under US stimulation, the S doping and oxygen deficiency induced higher electron transfer efficiency, significantly elevating the sonocatalytic ability. Furthermore, Ti-S-TiO_{2-x} exhibited promising sonotherapeutic and PTT antimicrobial performance on *S. aureus* with antibacterial efficiency of 99.995 %.

The combination of TiO_2 with noble metal has attracted extraordinary attention by enhancing the activity for bacteria reproduction inhibition. Thus, Liang et al. prepared a CuO_2/TiO_2 nanocomposite integrated hyaluronic acid hydrogel as an integrated microneedle for wound healing [72]. In another case, Sun et al. devolved Au nanoparticle-modified TiO_2 nanotubes for bare titania surface modification (Au NPs-TNTs), leading to the *P. gingivalis* inhibition [73]. To improve the quantum yield SDT effect of TiO_2-based sonosensitizers, the modification with functional polymer on TiO_2 can significantly increase ROS production rate or achieve the synergistic antibacterial activity. In a recent study, Cheng et al. designed polydopamine-coated mesoporous TiO_2 ($mTiO_2$@PDA) with PTT/SDT/PDT with antimicrobial function (Fig. 3**B**) [74]. The results showed that the temperature of $mTiO_2$@PDA raised by 25 °C under a near-infrared laser (NIR) power at 2 W/cm^2 for 6 min, and displayed great ROS generation ability under US treatment (1.5 W/cm^2, 3 MHz) for biofilm structure destroying.

4.2. BTO-based nanoplatforms

BTO is a piezocatalysis material with a high dielectric constant that exhibited excellent piezoelectricity, ferroelectricity, and acceptable biocompatibility [75]. Liu et al. fabricated BTO nanoparticles with a tetragonal phase, followed by hydrothermal synthesis of cubic phase BTO nanoparticles and calcination treatment at 800 ℃ for 10 h, resulting in BTO nanoparticles with excellent piezoelectric catalytic effect [76]. Injectable hydrogels based on oxidized hyaluronic acid were also introduced in this multifunctional platform (BT-OHA/THM-APMH hydrogel) to adsorb exudate in wound site and hinder bacteria invasion.

Nevertheless, the antibacterial efficacy of BTO is insufficient compared with antibiotics. To solve this problem, researchers have designed different nanostructures or combined new therapy strategies for enhancing the BTO-based SDT antibacterial performance. For instance, Zhu et al. developed a core–shell nanostructure using barium titanate (BTO) and zeolitic imidazolate framework-8, together with the additional loading of ciprofloxacin (BTO@ZIF-8/CIP) [77]. In this system, this nanoplatform exhibited a remarkable SDT effect for bacterial inhibition at the preliminary stage; the bacteria-killing rate against *S. aureus* was higher than 99 %. Based on BTO and ZIF-8 core–shell structure, CIP and Zn^{2+} released and ROS level decreased by SDT-associated degradation of ZIF-8 under an acidic environment. BTO@ZIF-8/CIP with heterostructure could eliminate bacteria at the initial stage and dynamically change under an acidic microenvironment to effectively accelerate wound healing.

In another way, He et al. designed a barium titanate with controlled oxygen vacancy (Vo-BTO) by thermal reduction treatment to enhance ROS generation ability [78]. Furthermore, Lei et al. reported a novel nanoparticle with bacterial elimination activity based on sulfur-doped oxygen-defective BTO (SDBTO) for osteogenic therapy [79]. The unique sulfur doping structure increased crystal asymmetry and reduced

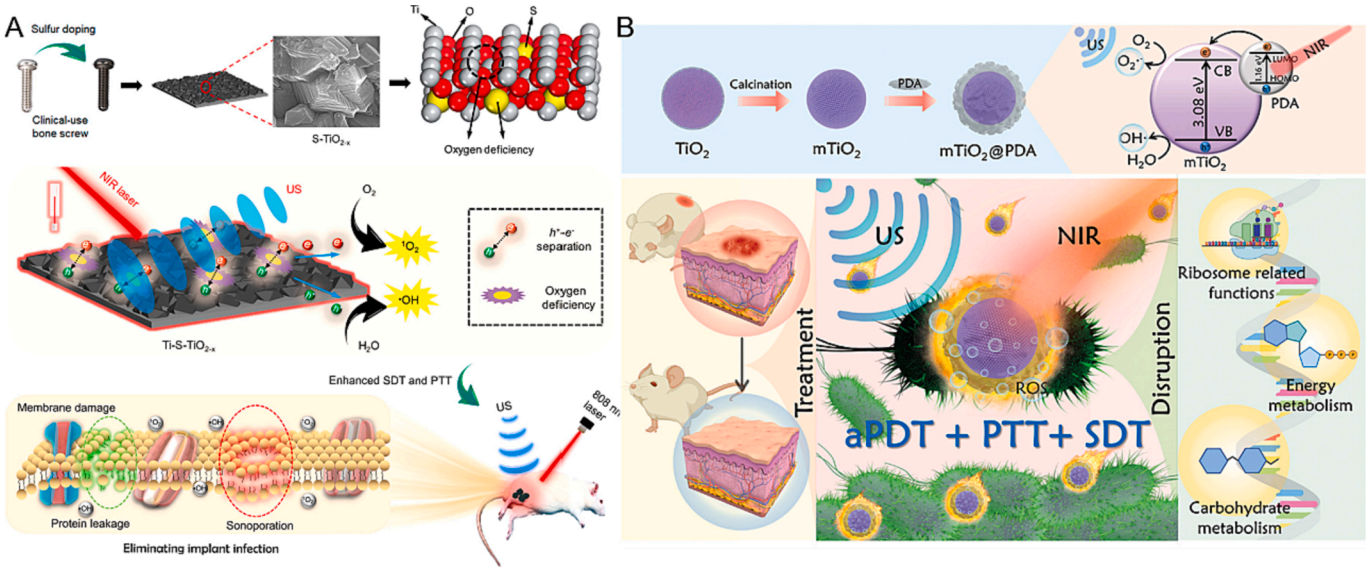

Fig. 3. (A) Schematic illustration that shows the sulfur-doped clinically used bone screw has enhanced sonocatalytic-PTT ability by creating oxygen deficiency and exhibits efficient bone infection therapy. Reproduced with permission [71]. (B) Schematic illustration of NIR/US triggered $mTiO_2$@PDA for PDT/PTT/SDT synergistic antibacterial effect. Reproduced with permission [74].

electron-hole pair recombination, thus showing excellent piezoelectric performance. In this therapeutic system, SDBTO can generate a piezoelectric electric signal under mild US and boost osteogenic differentiation by upregulating transforming growth factor-β (TGF-β) pathway. As a result, SDBTO-1 displayed an *S. aureus* inhibition rate of 97.12 %, which was 5.6 times higher than BTO group, significantly promoting osteogenesis in the infectious bone defect model. In addition, piezoelectric/metal heterostructure on sonocatalytic antibacterial therapy was reported by Wu et al., and ultra-small Au nanoparticles were chemically reduced into BTO to form Au@BTO nanocomposite [80]. The constructed nanocomposites demonstrated high-efficient sonodynamic treatment towards *S. aureus*-infected wounds. Under US irradiation, the nanocomposites displayed an enhanced •OH and $^1O_2$ generation effect *via* redox reactions. It should also be noted that the generated ROS based on the SDT process showed high antibacterial efficiency and boosted the migration of fibroblasts and macrophages.

4.3. Molybdenum-based nanoplatforms

Molybdenum-based nanomaterials, including molybdenum disulfide, MoO_2, and MoO_3, can be utilized for antibacterial application due to the NIR absorption properties [81]. Recently, Mo-based semiconductor materials have acted as sonocatalysts for ROS generation under US irradiation. For instance, Chen et al. synthetized two-dimensional MoS_2 nanosheets with different crystal phase and then investigated the crystal phase-dependent SDT activity [82]. In detail, compared with the semiconducting 2H-phase, 1T/1Ť phase MoS_2 enhanced the US-induced generation of ROS. It's worth noting that the SDT-induced antibacterial activity of M-MoS_2 is further enhanced by the PTT performance with 1064 nm laser treatment. *In vivo* results demonstrated that the M-MoS_2 integrated PTT-enhanced SDT for antibacterial therapy. In another work, Feng et al. developed a bifunctional sonosensitizer based on MoS_2 quantum dots decorated porphyrin-like Zn single-atom nanoplatform (g-ZnN_4-MoS_2) *via* electrostatic interactions [83]. The heterogeneous interfaces of nanoplatform had a high interface charge transfer activity, which showed the most excellent sonocatalytic performance. Under US irradiation, the as-prepared g-ZnN_4-MoS_2 could not only improve the interfacial charge transfer, but also reduced the activation energy of O_2 for effective $^1O_2$ generation.

Novel molybdenum-based nanomaterials have the unique potential to be clinically translated for bacterial infectious disease treatment. Zhou et al. synthesized $MoSe_2$ nanoflowers ($MoSe_2$ NF) for biofilm eradication under the control of the US with maximum biosafety [84]. Notably, $MoSe_2$ NF possessed outstanding piezoelectricity based on the great curvature and sufficient surface area, which also exhibited glutathione oxidase-mimic and peroxidase-mimic activity under biofilm microenvironment. Moreover, the surface coating of poly(ethyleneimine) (PEI) improved the antioxidative of $MoSe_2$ NF and proved the potential of nanoplatform in bacterial biofilm eradication. For a more effective paradigm, He et al. reported sodium molybdenum bronze nanoparticles (SMB NPs) for synergistic SDT under US irritation and PPT under the second near-infrared treatment [85]. The SMB NPs were produced from molybdenum trioxide nanobelts by hydrothermal method and then enhanced oxygen vacancy density and widen interlayer gaps. With the help of high second near-infrared treatment absorbance of SMB NPs, such nanoplatform could efficiently promote ROS generation and display remarkable PTT inhibition against *S. aureus* and *E. coli* cells. In another effective paradigm, Zong et al. demonstrated a network-like structure constructed by MoOx in situ on Mo_2C MXene (MoOx@Mo_2C) [86]. Layered ternary molybdenum gallium carbide (Mo_2Ga_2C) bulky precursor was etched with HCl and then reacted under 140 °C to produce Mo_2C MXene with single- and few-layered structures. The MoOx@Mo_2C composites were obtained by moderate oxidation and then encapsulated with polyvinyl pyrrolidone. Considering the high sono-sensitizing efficiency, this nanonetworks displayed significant and efficient pathogenic bacteria repression under US irradiation. Moreover, the nanonetworks showed excellent bacteria capture activity due to the intense interaction between MoOx@Mo_2C and bacteria, which benefits in killing pathogenic bacteria more efficiently.

4.4. Carbon-based nanoplatforms

Carbon-based nanoplatforms with exceptional structural characteristics and distinguished physicochemical properties have demonstrated their activity against tumor and bacteria-associated infections [87,88]. Transition metal carbonitrides (MXenes) have been developed over a decade ago. However, these materials have been recently applied for medical applications, achieving the SDT effect for efficient tumor therapy and bacterial infection treatment [89]. For example, Ma et al. developed a lattice-strain-rich Ti_3C_2 using Ti_3C_2 and TCPP as raw materials by solvothermal method [90]. The addition of TCPP narrowed the band gap of Ti_3C_2, promoting ROS production by accelerating the US-induced electron-hole pair separation and facilitating electron transfer.

Mao et al. reported a novel 2D catalytic planar defected in Ti_3C_2 [Ti_3C_2-SD(Ti^{3+})] sheets with neutrophil membrane proteins modification (NM-Ti_3C_2-SD(Ti^{3+}) for MRSA-infected bony tissue healing [91]. The abundance of Ti^{3+} species in the Ti_3C_2 sheet facilitated the activation of O_2 and showed superior $^1O_2$ generation activity under US stimulation. Accordingly, these innovative nanosheets in the presence of US treatment efficiently eliminated MRSA-induced bone infection with an inhibition rate close to 100 % (99.72 % ± 0.03 %), alleviating tissue inflammation and showing excellent bone-repairing abilities. In another work, Yu et al. constructed CaO_2-loaded 2D Ti_3C_2 nanosheets to increase ROS production in response to US treatment [92]. CaO_2 nanoparticles induced the oxidation of MXene to generate TiO_2 for SDT, and produced ·OH and O_2 via the Fenton reaction to induce bacterial death. To increase the antibacterial efficiency, Li et al. proposed an antibacterial platform based on the bismuth ferrite-functionalized 2D Ti_3C_2 nanosheets ($BiFeO_3$/Ti_3C_2) based on electrostatic interaction that integrated a synergistic PTT and SDT effect [93]. In detail, US stimulation-derived the ferroelectric polarization of $BiFeO_3$/Ti_3C_2 and the production of cavitation bubbles, which may lead to thermal impacts and luminescence. More importantly, combining the Schottky junction and ferroelectric polarization significantly enhanced ROS yield. After 20 min of US stimulation, $BiFeO_3$/Ti_3C_2 could eradicate bacteria-induced osteomyelitis effectively.

Similarly, Bai et al. designed a nanoplatform with heterostructure that was constructed by zinc oxide nanorod and two-dimensional carbon nanomaterial graphdiyne nanosheet (ZnO@GDY) by solvothermal method and self-assembled method [94]. When combined US irradiation with H_2O_2 exposition, the bacteria killing rate of ZnO@GDY was enhanced higher than 99.999 % for MRSA and *P. aeruginosa* due to the piezoelectric property and the nanozyme activity.

To alleviate inflammation in the wound healing process, Shi et al. constructed graphitic carbon nitride nanosheets and then modified with platinum-ruthenium nanoalloys (PtRu/C_3N_5) as a piezoelectric and photocatalytic nanozyme-based antibacterial system for eliminating bacteria and inhibit inflammation reactions [95]. In the synergistic antibacterial approach, C_3N_5 nanosheets were not only used as a piezoelectric material for ROS generation but integrated PtRu for hydrogen (H_2) gas generation and oxidase -like activity enhancement. Furthermore, hyaluronic acid microneedles were used to coat PtRu/C_3N_5 for accelerating MRSA-infected wound healing. Benefiting from the combination of ROS with US treatment and H_2 by photocatalysis, the multifunctional platform provided a competitive strategy for antibacterial and anti-inflammatory.

4.5. Noble metals-based nanoplatforms

Noble metals-based nanoplatform, including metal peroxide nanoparticles, metal oxides nanoplatform, metallic nanoparticles, and metal nanocomposites, have been considered efficient sonosensitizers with

superior characteristics. As a typical paradigm, Lu et al. fabricated Ag nanoparticles loaded P18-PEG polymer (PEG-P18-Ag NPs) as a promising nano-sonosensitizer for SDT [96]. The US-triggered ROS generation and Ag^{+} releasement significantly upregulated the cell envelope, ribosomes, and chromosomes-related gene expression, resulting in significant antibacterial effects in MRSA-induced infection.

For enhancing the antibacterial activity of SDT, Bi et al. designed Ag_2O_2 NPs as a novel stimuli-responsive antibacterial nanoparticle for SDT and PTT therapy [97]. Recently, Cheng et al. developed novel sonosensitizers based on PEG-coated platinum-copper nanoparticles (PtCu-PEG NPs) for efficient bacterial elimination [98]. In detail, PtCu-PEG NPs showed excellent broadband bacteria-killing ability by SDT performance, Fenton-like catalytic, and glutathione depletion activity. Furthermore, PtCu-PEG NPs promoted angiogenesis by up-regulating the hypoxia-inducible factor-1 (HIF-1α), platelet endothelial cell adhesion molecule 31 (CD 31) level, which could also increase the M1 & M2 macrophage level for bacteria elimination. Under US irradiation, PtCu-PEG nanoplatform-mediated SDT and glutathione-enhanced chemodynamic therapy-mediated combination therapy successfully eradicated osteomyelitis.

Nanocomposite with heterostructure was proven to be a desirable SDT agent due to electronic structure modulation. For instance, Zhu et al. fabricated Au nanoparticles incorporated Cu_2O nanocube (Au@Cu_2O) as a nano sonosensitizer, which exhibited excellent SDT antibacterial performance by enhancing the oxidative stress level and disrupting bacterial membrane [99]. Integrating nanoparticles with 3D structure hydrogel as a composite material can improve the properties of the components. Likely, Tao et al. obtained stanine nanosheets using the liquid-phase exfoliation method and coated them with PEI, and then assembled them with polymer poly(d,l-lactide)-poly(ethylene glycol)-poly(d,l-lactide) for hydrogel formation (Sn@hydrogel) [100]. It is worth mentioning that MRSA count of Sn@PEI treatment groups was 63.4 %, after exposure to US and Sn@PEI treatment, the survival of MRSA was significantly decreased to 0.5 %. In addition to bacteria-killing activity, the Sn@hydrogel has exhibited thermosensitive and injectable behavior, which was suitable for bacteria infected wound healing promotion.

Similarly, Zheng et al. reported a thermosensitive chitosan hydrogel for CuO_2 nanodots and L-Buthionine-(S, R)-sulfoximine loading (CuO_2-BSO@Gel) [101]. CuO_2 nanodots could further produce ROS as a semiconductor material under US irradiation. More importantly, the CuO_2 nanodots with the capability of catalyzing H_2O_2 to produce •OH and also induced O_2 generation for SDT effect enhancement. This composite-based chemo-SDT antibacterial therapy strategy could significantly accelerate the *S. aureus*-infected wound healing and efficiently tumor growth inhibition.

4.6. Metal-organic framework (MOF)-based nanoplatforms

MOFs are porous materials composed of metal ions and organic linkers, which have attracted considerable interest in antibacterial agent delivery due to the high specific surface area and tunable pore size for ultra-high drug loading [102]. Besides, MOF-based nanoplatforms possess outstanding antibacterial effects due to their unique chemical structure for releasing related metal ions [103]. Moreover, MOF-based nanoplatform encapsulated with sonosensitizers and metal ions has been verified to be a nano-sonosensitizer with higher SDT effect based on the US-triggered charge separation. Porphyrin-based MOFs outstand from the conventional sonosensitizer-loaded MOF nanoplatform, which prevented the self-quenching and aggregation of porphyrin and improved the ROS generation effect of SDT [104]. Zeng et al. reported porphyrin-based MOF with homojunction structures (D-PCN-2) by using acetic acid and benzoic acid as modulators, which significantly enhanced the ROS production effect by improving the electron-hole pairs separation activity (Fig. 4**A**) [105]. The obtained results demonstrated that D-PCN-2 promoted the elimination of MRSA with US irradiation, showed excellent acceptable biocompatibility, and produced benefits for osteomyelitis treatment.

Besides improving the SDT effect of MOFs, functional nanomaterials such as metal nanoparticles or surface modification have also been used for enhancing SDT activity. Meng et al. utilized silver nanoparticles modified Ti-based MOF to achieve ROS generation for SDT efficacy with

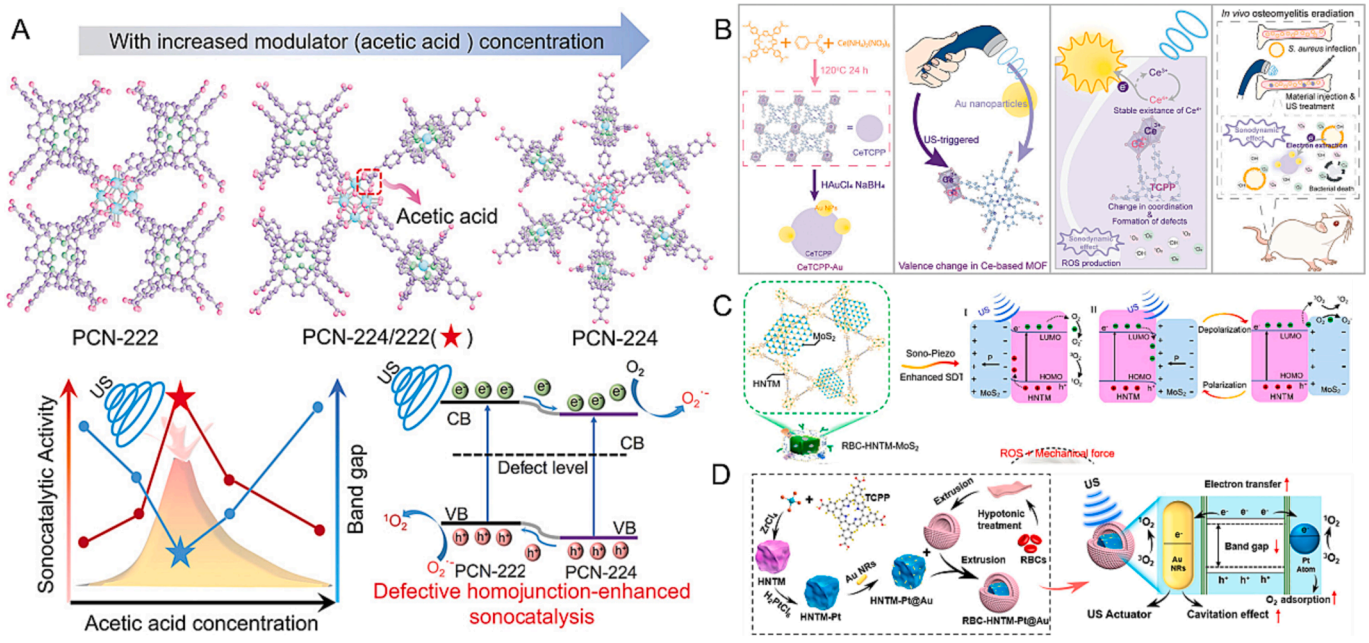

Fig. 4. (A) The transformation process of MOF crystal structure with the increase of acetic acid concentration and the corresponding defect-enhanced sonocatalytic mechanism. Reproduced with permission [105]. (B) Schematic illustration of CeTCPP-Au for US-triggered electron trapping of Au NPs on CeTCPP for defect engineering. Reproduced with permission [107]. (C) Sonocatalytic mechanism of HNTM-MoS_2 and the efficient SDT treatment of osteomyelitis through rapid MRSA elimination and detoxification. Reproduced with permission [110]. (D) Synthesis of the RBC-HNTM-Pt@Au and the treatment of osteomyelitis through efficient SDT. Reproduced with permission [111].

bacterial infection eradication and tumor growth inhibition (MIL@Ag-PEG) (Fig. 4**B**) [106]. The electrochemical experiments demonstrated that the doped nanoparticles enhanced the charge transfer efficiency significantly and then decreased the oxygen adsorption energy, resulting in the highly ROS generation effect. Similarly, Zheng et al. prepared by Ce^{3+}/Ce^{4+} coordinating with tetrakis(4-carboxyphenyl) porphyrin (TCPP) (CeTCPP) and then employed cerium-based MOF for Au nanoparticles loading (CeTCPP-Au) (Fig. 4**B**) [107]. Compared with CeTCPP, CeTCPP-Au facilitated electron-hole separation with the help of Au nanoparticles. In detail, Au nanoparticles activated the valence change of Ce^{3+} to Ce^{4+} through electron trapping. Thus, they caused structural irregularity of CeTCPP, resulting in a higher generation of ROS under the SDT process. Guo et al. synthesized NIR-driven nanomotors based on gold deposited on the half surface of MOF, which were modified with DNase I (MOF@Au-DNase I) for biofilm eradication [108]. The MOF@Au-DNase I sample showed remarkable photothermal properties under NIR laser irradiation. Moreover, the motion of nanomotors significantly facilitated the contact between nanomotor and bacteria. Benefiting from the asymmetric spatial distribution of Au in nanomotor, the ROS generation efficiency was significantly enhanced to eliminate of biofilms. In another work, Wang et al. synthesized porphyrin-based-MOFs modified Nb_2C hybrid nanomaterials (HNTM/Nb_2C) to enhance the SDT effect [109]. In this platform, porphyrin-based-MOF could be a useful material for the abundant generation of electron-hole pairs, in which Nb_2C in this Schottky heterojunction achieved rapid charge transfer, significantly improving ROS production under US treatment.

To improve the biosafety of nanoMOF, Feng et al. synthesized multifunctional core–shell MOF to improve the sonocatalytic ability and enhance the biocompatible of porphyrin-based MOF (Fig. 4**C**) [110]. Among them, MoS_2 nanosheets loaded with porphyrin-based hollow MOF acted as cores, and the red cell membrane worked as the shell (RBC-HNTM-MoS_2). As a piezoelectric material, MoS_2 nanosheets improved the charge transfer of nanoMOF and enhanced ROS production. It is noteworthy that ROS-based piezoelectric-assisted sonocatalysis and strong mechanical force triggered by the US successfully eliminated the bacterial infection of bone tissue. In another study, Yu et al. prepared Pt single atoms immobilized zirconium-based porphyrin MOF nanoplatform for loading Au nanorods (HNTM-Pt@Au) (Fig. 4**D**) [111]. After being coated, biocompatibility and toxin-neutralization ability was improved. Importantly, combining Pt single atoms in a nanoplatform might decrease the energy barrier for sonocatalytic ability enhancement of porphyrin-based MOF. *In vivo* results proved that RBC-HNTM-Pt@Au efficiently achieved SDT therapy on *S. aureus*-infected osteomyelitis based on single-atom catalysis.

5. Applications of SDT in bacterial infectious diseases

5.1. Skin infection

Due to the nourishing environment of the damaged wound for pathogenic bacteria growth, bacterial wound infection has high morbidity in clinics, posing enormous and arduous challenges to human health [119]. Conventional antibiotics showed undesired bactericidal effects due to the antibiotic resistance of bacteria and the highly complex structure of the biofilm microenvironment [120]. Nanoplatform-based SDT strategies for bacterial-infected wound healing have attracted much attention for their antibacterial function with profound penetration effect [68].

However, the therapeutic effects of SDT were limited due to the hypoxic microenvironment in infected wounds, and O_2 was rapidly depleted during the SDT process. In response to the challenge, Bi et al. synthesized Ag_2O_2 NPs for killing bacteria and destroying bacterial biofilms [97]. Ag_2O_2 NPs exhibited self-supply of H_2O_2 and O_2 ability for inducing oxidative stress while providing a sustained release of Ag^+. Meanwhile, this nanoparticle featured US-assisted ROS production activity and attractive PTT properties for effective wound healing performance. Similarly, Liang et al. constituted a heterostructure composed of oxygen vacancy-rich TiO_2 nanosheets and copper peroxide nanoclusters (CuO_2/TiO_2) and then integrated into hyaluronic acid microneedle patch (CTMN) [72]. As a result, CuO_2/TiO_2 generated excess ROS for bacteria-killing, which could reduce the recombination ratio of electron and hole pairs effectively under US irradiation. Besides, CuO_2/TiO_2 with efficient sonothermal conversion efficient and excellent O_2 generation activity by catalyzing hydrogen peroxide to alleviate SDT-induced hypoxia. CuO_2/TiO_2 achieved excellent drug-resistant pathogens killing rate (> 99 %) based on SDT and chemodynamic effect, which also displayed efficient self-supplying O_2 for ameliorating hypoxia and accelerated the bacterial infections wound healing process. Moreover, CTMN resulted an outstanding therapeutic effect on MRSA-infected wounds by ameliorating inflammation responses, leading to lower levels of interleukin-6 (IL-6) and tumor necrosis factor-α (TNF-α) (Fig. 5).

Besides the enhanced ROS generation capability, cellular migration and tissue regeneration are also essential steps in bacterial-infection wound healing. Incorporating ions such as Zn^{2+} offers combined advantages to improve antimicrobial activity and accelerate the wound healing process because it could up-regulate metallothioneins and increase the proliferation of skin fibroblasts [121]. Zhu et al. designed a dynamically evolving piezoelectric nanocomposites named BTO@ZIF-8/CIP by introducing the Zn^{2+} for fibroblast proliferation promotion [77]. Results showed that the proper ROS with a lower level, piezoelectric signal, and Zn^{2+} releasement could promote fibroblast migration and improve tissue regeneration. As confirmed by cell migration analysis, SDT-induced low ROS level and piezoelectric signal could promote the migration of fibroblasts to accelerate the wound healing process. In another work, Xiang et al. reported a zinc porphyrin-based MOF and ZnO nanocomposite (ZnTCPP@ZnO) embedded hyaluronic acid-based microneedle patch for acne treatment [122]. Because of its SDT-based antibacterial ability of ZnTCPP@ZnO, and 99.73 % *Propionibacterium acnes* cell-killing ratio was obtained when the US exposure time was extended to 15 min. Gene ontology (GO) and the kyoto encyclopedia of genes and genomes (KEGG) results showed that DNA replication-related genes such as Rfc4, Rfc3, Lig1, Mcm6, Dut, and Dctcpp1 were up-regulated with ZnTCPP@ZnO treatment for promoting the proliferation of fibroblasts.

To promote angiogenesis using growth factor, Huang et al. designed Au nanoparticles-BTO nanoplatform attached Janus piezoelectric patches for a vascular endothelial growth factor (VEGF) loading using three-dimensional (3D) printing technology [123]. In their work, the Janus hydrogel patch was constructed by Au nanoparticles-BTO nanoplatform-loaded poly (ethylene glycol) diacrylate (PEGDA) and the VEGF-loaded gelatin methacryloyl (GelMA), which was divided into top and bottom structure. Therefore, VEGF functionalization of Janus piezoelectric patches was expected to inhibit cell growth, increase collagen deposition and decrease TNF-α expression, achieving an effective SDT-based antibacterial property and angiogenic efficacy. Immunostaining analysis of alpha-smooth muscle actin and CD 31 also revealed the formation of vascular structures at large amounts in the group that received Janus patch with US treatment.

However, an ideal wound dressing for bacteria-infected wound healing should protect the wound from bacteria while facilitating cell proliferation and tissue remodeling to speed up wound healing. It is essential to utilize combination strategies to heighten the stability and biocompatibility of nanoplatform for further biomedical application. The utilization of the nanoparticles-deposited hydrogel-based superstructures is a promising strategy in the biomedical area [124]. More importantly, the advanced properties of the hydrogel, such as adhesive, injectable and self-healing properties, construction of the nanosonosensitizer composited hydrogel with multifunctional also improved the wound healing in infected wound sites. For example, Liu et al. fabricated an injectable hydrogel with self-healing and adhesive capacity (BT-oHA/THM-APMH) based on barium titanate nanoparticles

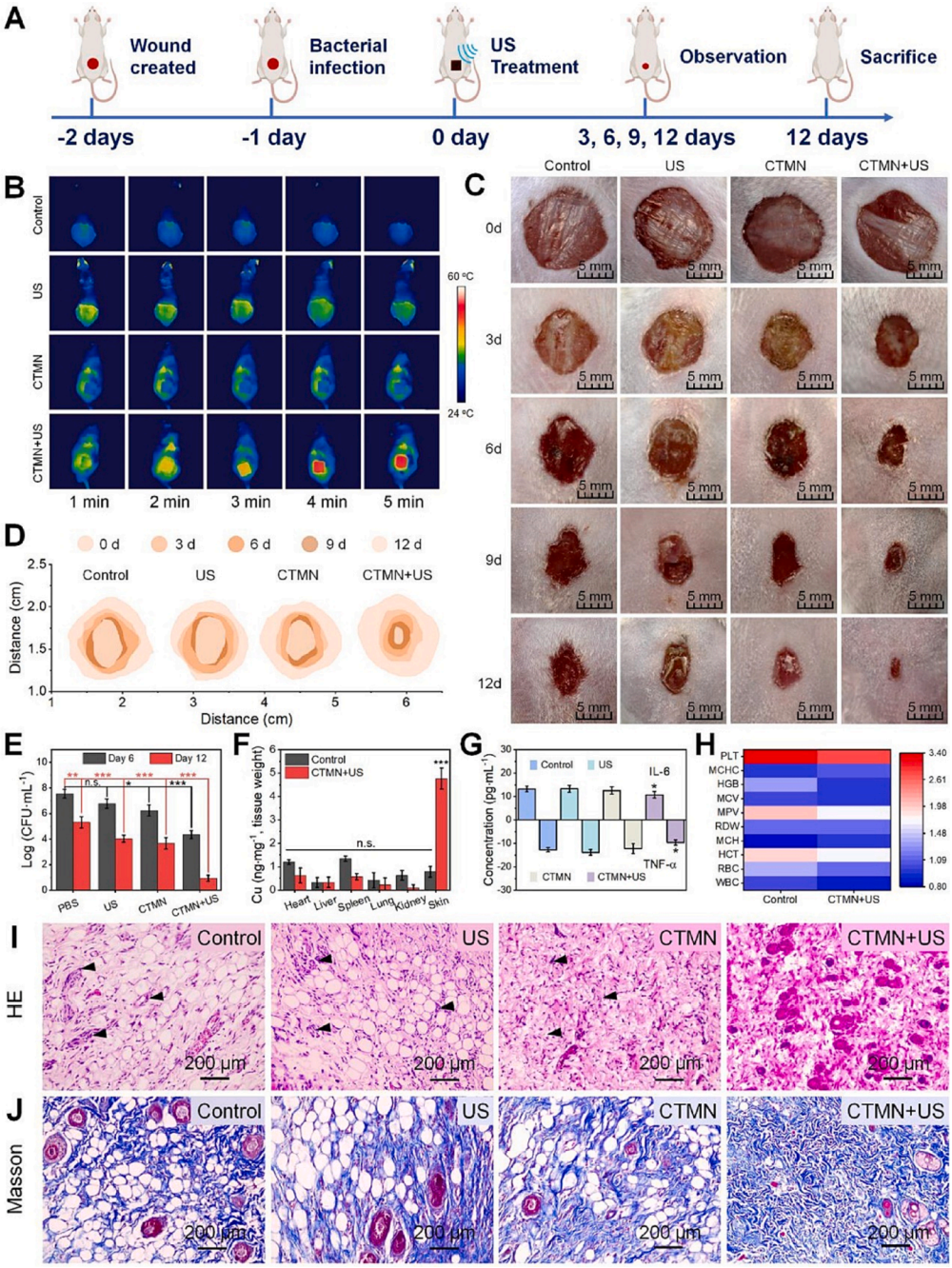

Fig. 5. *In vivo* therapeutic performance of CTMN. (A) Schematic diagram of treatment strategy in the MRSA-infected murine wound model. (B) Thermal images of the CTMN treated wound under US (1.0 W/cm^2, 1 MHz) at varied time intervals. (C) Representative images of wounds infected with MRSA in different groups on days 0, 3, 6, 9, and 12. (D) Traces of chronic wound closure over 12 days upon different treatments. (E) Bacterial viability of the wounded tissues. (F) Accumulation of Cu^{2+} ions in different tissues of mice. (G) IL-6 and TNF-α levels. (H) The blood test panel of mice after 12 day treatment. (I) H&E and (J) Masson staining of the wounded tissues upon different treatments. Reproduced with permission [72].

and oxidized hyaluronic acid (oHA) and N-(3-aminopropyl) methacrylamide hydrochloride grafted N-[tris(hydroxymethyl)methyl] acrylamide (THM-APMH) [76]. BT-OHA/THM-APMH hydrogel triggered by the US exhibited excellent inhibition activity of *E. coli* and *S. aureus*. In addition, it improved the migration of mouse embryonic fibroblast (NIH-3T3) cells by remarkably increasing the epidermal growth factor (EGF), basic fibroblast growth factor (bFGF), VEGF, type I collagen (COL-I), and type III collagen (COL-III) expression. Animal experiments further demonstrated that BT-OHA/THM-APMH hydrogel + US significantly up-regulated the level of VEGF, CD 31, and α smooth muscle actin (α-SMA); down-regulated the level of IL-10 and TGF-β. This synergistic strategy combining nanoparticles with SDT antibacterial activity embedded multifunctional hydrogels has provided a new perspective with clinical significance for wound healing.

5.2. Osteomyelitis

Osteomyelitis is an intractable orthopedic disease associated with disability or severe sepsis caused by the invasion of pathogenic microorganisms in bone tissue [125]. Due to ischemic sclerosis in the diseased microenvironment and insufficient blood supply in soft tissue, high-dose antibacterial agents were required to achieve appropriate concentration

for bacterial killing [126]. The overuse of antimicrobial drugs in clinical has been reported to exhibit severe systemic toxicity and promote the emergence of drug resistance [127,128].

Encouraged by the excellent tissue-penetration depth of US and the non-invasiveness during the treatment, SDT shows distinct potential to replace antibiotics treatment and avoid the multiple surgical debridements against osteomyelitis [129,130]. Cheng et al. reported gold-doped titanate nanotubes conjugated with guanidinium-rich polymer (Au/TNT@PG) for MRSA biofilm elimination by SDT [113]. The peroxidase-like activity of nanocomposite enabled the generation of •OH at the infection-microenvironment towards SDT, and the strong affinity of polymer to microbial membranes improved the penetration within the biofilm matrix. The sonodynamic-catalytic therapy effectively eradicated planktonic bacteria and disrupted biofilms implying an innovative synergistic strategy for treating MRSA-infected osteomyelitis.

Due to the immunoregulation and osteogenesis promotion playing a pivotal role in osteomyelitis treatment, novel antimicrobial nanomaterials for inducing bone regeneration have been designed for adjuvant SDT of osteomyelitis. Recently, Wang et al. synthesized a porphyrin-based-MOF modified Ti_3C_2 hybrid nanomaterials (HNTM/Ti_3C_2) for enhancing the SDT effect [117]. Based results of the protein and gene expression in human bone marrow mesenchymal stem cells (hBMSCs), it was demonstrated that the HNTM/Ti_3C_2 significantly upregulation the osteogenesis-related protein expression levels of alkaline phosphatase (ALP) and osteopontin and enhanced the runt-related transcription factor 2 (RUNX2), osteopontin, ALP, BMP2, COL-1, and osteocalcin genes expression level. RNA sequencing results demonstrated that the synergistic effect could significantly improve bone regeneration by activating the calcium, mitogen-activated protein kinase, and Wnt signaling pathways. The finally obtained nanocomposite has shown apparent effectiveness for treating MRSA-infected osteomyelitis by SDT.

Since Zn^{2+} with the ability to promote the osteogenic differentiation, Feng et al. synthesized a multifunctional SDT nanoplatform based on g-ZnN_4-MoS_2 for MRSA-infected osteomyelitis (Fig. 6) [83]. The MRSA membrane deformation in response to the g-ZnN_4-MoS_2 administration upon US irradiation and bacterial killing efficiency was also demonstrated to be 99.58 % *in vitro*. Moreover, the fixed Zn single-atom in nanoplatform provided a sustained release of Zn^{2+} in 28 days with

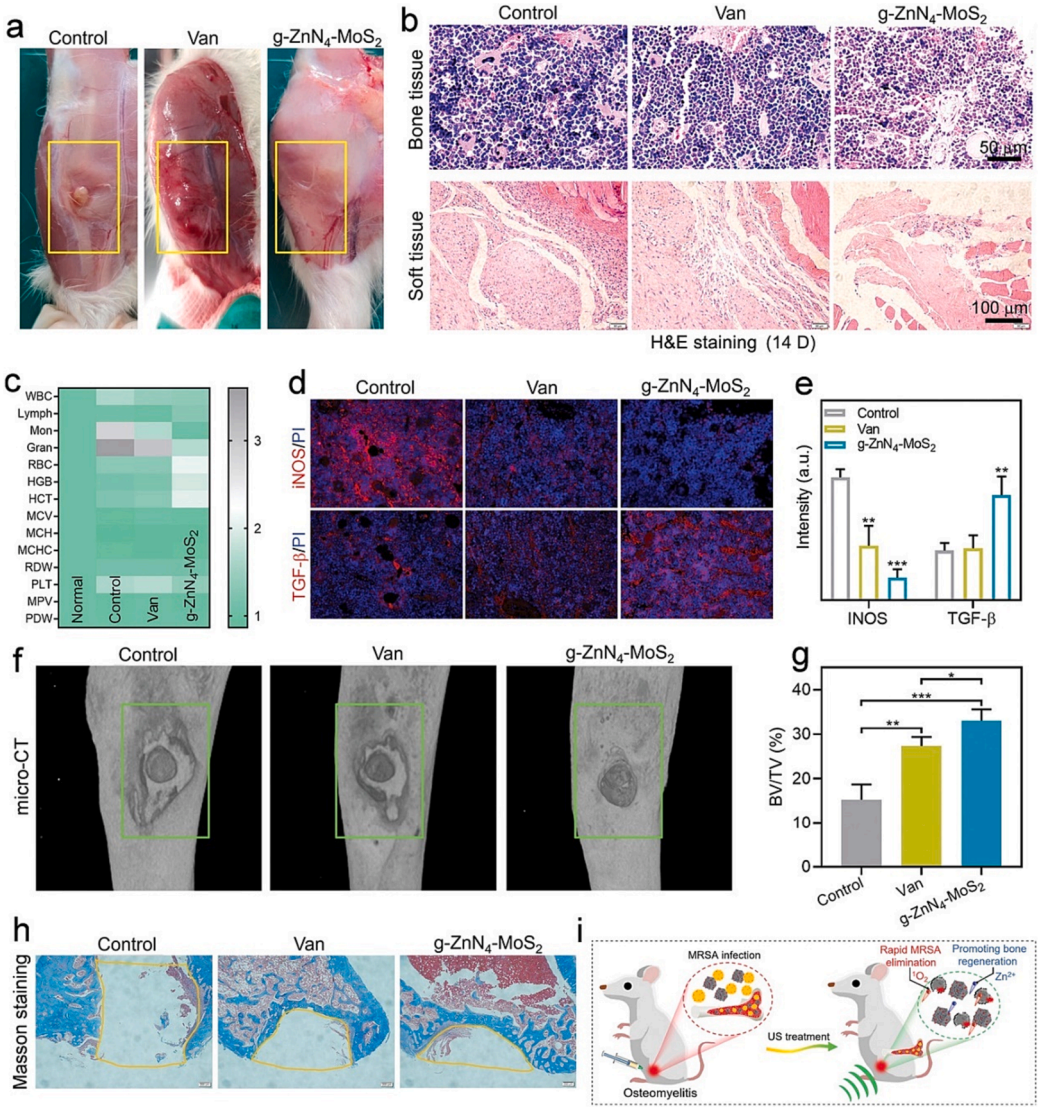

Fig. 6. g-ZnN_4-MoS_2 mediated SDT for osteomyelitis *in vivo*. (A) Wounds of infected legs. (B) H&E staining of bone narrow and surrounding tissue, (C) Routine blood results. (D) Immunofluorescent staining, (E) Related fluorescence intensity statistics of inducible nitric oxide synthase (iNOS) and TGF β in the bone narrow tissue. (F) Micro-CT analysis and (G) BV/TV results of the infected legs. (H) Masson staining of the infected bone defects. (I) Illustration of SDT for osteomyelitis. Reproduced with permission [83].

effective concentration for promoting osteogenic differentiation. The results of osteogenic-related gene expressions showed that g-ZnN_4-MoS_2 enhanced the level of ALP, RUNX2, and COL-1 of MC3T3-E1 cells. The protein expression results also proved that g-ZnN_4-MoS_2 could enhance RUNX2 and osteocalcin expression. Moreover, the micro-computed tomography (micro-CT) and the bone volume/total volume (BV/TV) results of the bone defect sites indicated the above-mentioned g-ZnN_4-MoS_2 showed more effective bone repair ability.

5.3. Implant infection

Implant-related infection is the major risk factor and complex problem that causes of failure of orthopedic implants in clinical [131]. Getting rid of implant-related infection are treated with surgeries by implant replacement, which will bring additional pain and economic pressure on patients [132]. Antibacterial coatings with nanoplatform have attracted lots of attention to solving implant infection problems. In addition, SDT has become a promising method to remove the biofilm implant infection with fewer side effects. Based on such grounds, Li et al. designed an Au-TiO_2 nanotubes nanoplatform (Au-TNT) with a heterojunction structure on the implant surface as a nanosensitizer for treating *peri*-implant infection [133]. The *in vivo* studies demonstrated that Au-TNT + US group could greatly enhance the inhibition rate (96.59 %) with fewer side effects. In addition, no alveolar bone loss and a few inflammatory cells were observed in the rat *peri*-implantitis model, revealing that implanted materials could achieve efficient bone repair properties *in vivo*.

Despite its successful application, the complicated hypoxia microenvironment still limits the SDT-based antibacterial efficiency. Fortunately, researchers have developed multifunctional nanoplatforms that could convert the US into thermal energy for sonothermal therapy. Guan et al. reported a metal-red phosphorus-coated Ti substrate and then modified with nitric oxide-precursor-loaded MSN nanoplatform (Ti-RP-SNO) to realize synergetic antibacterial effect [134]. Under continuous US excitation, Ti-RP-SNO could enhance more than 20 ℃, indicating its sonothermal effect for biofilm elimination. Together, the synergetic therapy based on sonothermal and NO treatments with Ti-RP-SNO elevated antibacterial performance compared with monotherapy, resulting in bone MRSA-associated infection elimination.

In addition to integrating SDT-antibacterial nanoparticles into the layers, the surface modification of the implant was also developed for combining PTT and SDT antibacterial therapy. As a typical paradigm, Zeng et al. modified the black phosphorus nanosheets and PDA on the Ti implants (Ti/PDA/BP) to achieve PTT-enhanced SDT [135]. GO classification of *S. aureus* with SDT treatment elucidated that the signaling pathways related with antioxidant and catalytic activity were both affected, and the KEGG results showed the metabolic system of *S. aureus* was also stimulated, referring to SDT induced antibacterial mechanism. Furthermore, *In vitro* results demonstrated that Ti/PDA/BP has good biocompatibility on bone regeneration-related cells and outstanding osteogenic differentiation property compared with Ti/PDA group and Ti group (Fig. 7). Consequently, it was found that Ti/PDA/BP-based PTT-

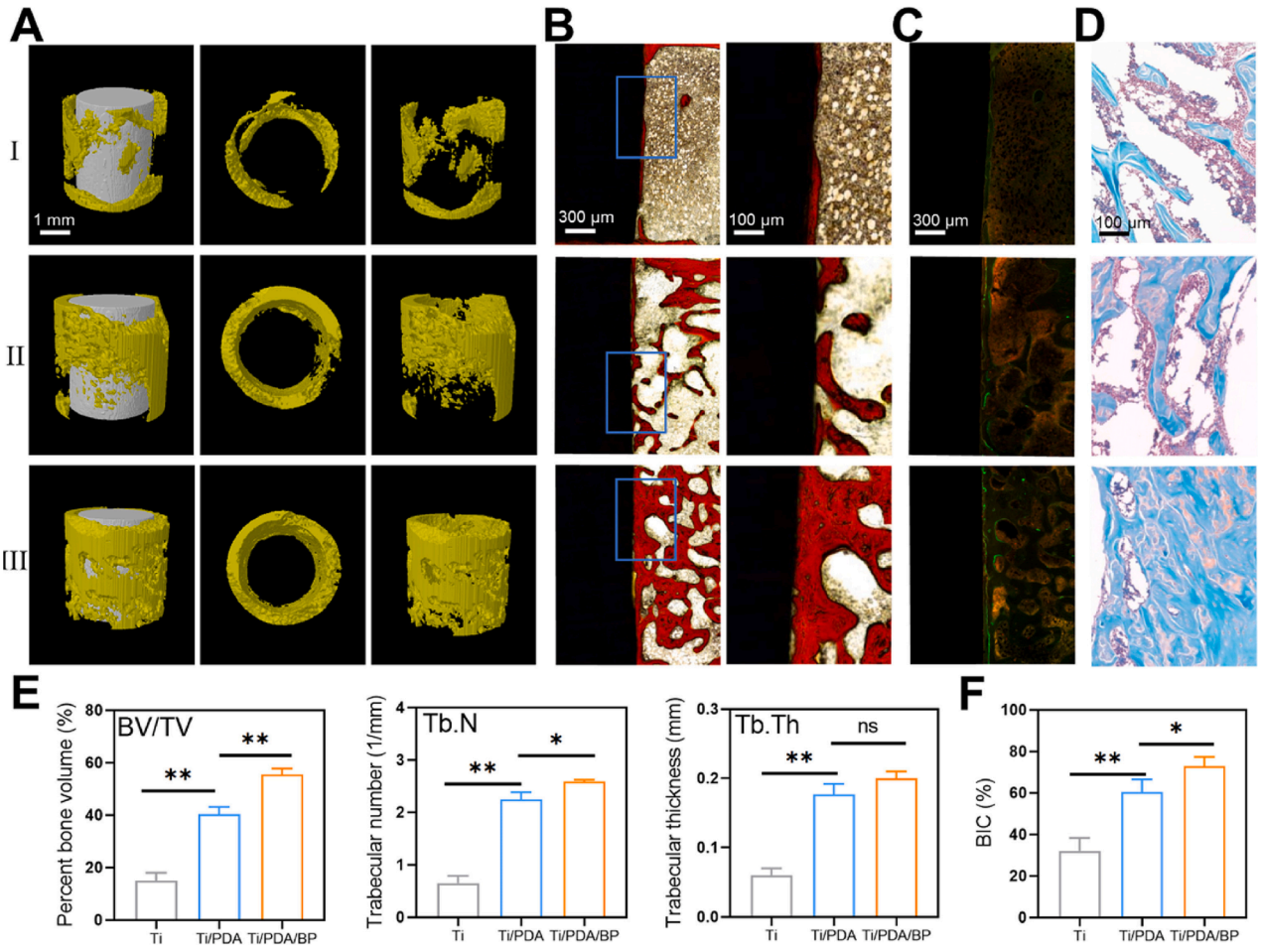

Fig. 7. Assessment of bone-implant osseointegration in Ti/PDA/BP (I: Ti; II: Ti/PDA; III: Ti/PDA/BP). (A) 3D reconstruction images of Micro-CT. (B) Representative images of Van Gieson staining. (C) Double labeling. (D) Safranin-O/Fast Green staining. (E) Quantitative analysis of BV/TV, trabecular number (Tb·N), and trabecular thickness (Tb·Th). (F) Percentages of bone-implant contact. Reproduced with permission [135]. (For interpretation of the references to colour in this figure legend, the reader is referred to the web version of this article.)

SDT antibacterial strategy was specifically higher than other groups *in vivo*, and it could effectively enhance the osseointegration of bone-implant.

5.4. Myositis

As a deep muscle infection by pathogens, bacterial myositis might cause generalized myalgia and multifocal myositis [136]. SDT for bacterial myositis treatment is an alternative to antibiotic therapy and surgical debridement that provides deeper tissue penetrability, higher safety, and excellent bacteria-killing efficiency.

Based on the enhanced permeability and retention (EPR) effect and electrostatic attraction between nanoparticles with infection site, Song et al. grafted Fe^{3+} and modified PEI on the surface of bismuth oxybromide nanoplates (Fe-BBP) to treat deep-seated MRSA-bacterial infection [137]. The Fe-BBP NPs could generate a burst ROS under US stimulation due to the Fe-mediated Fenton reactions in the H_2O_2-rich inflammation microenvironment and sonocatalysis effect. Flow cytometry experiments demonstrated that US-induced Fe-BBP NPs were shown to decrease bacterial membrane integrity and accelerate the ·OH production. Moreover, Fe-BBP NPs exhibited stronger accumulation in the MRSA-infected myositis after intravenous injection based on the positively charged surface compared with the control group, as well as acted as intelligent MRI contrast agents for bacterial infection diagnosis. Likewise, Su et al. modified *meso*-tetra(4-carboxyphenyl)porphine (T790) *via* PEG linker onto the surface of Pd@Pt nanoplates (Pd@Pt-T790) for bacterial myositis eradication (Fig. 8) [63]. As prepared Pd@Pt-T790 nanoplatform inherits catalase-like activity, it could be used as an accelerator of SDT by catalyzing O_2 generation to enhance antibacterial therapeutic. Due to the EPR effect, this novel nanoplatform could effectively accumulate in the infection site after intravenous injection. Importantly, Pd@Pt-T790 with excellent MRI and photoacoustic (PA) imaging activity for noninvasively monitoring SDT therapeutic progress, achieving outstanding antibacterial activity in an MRSA myositis model.

To further realize a targeted antibacterial and enhancement of bacteria-induced myositis site enrichment efficiency, targeting molecules were used to modify on the surface of nanoplatforms. Pang et al. designed a nanoliposome based on maltohexaose-modified cholesterol and 1,2-dioctadecanoyl-*sn*-glycero-3-phospho-(10-*rac*-glycerol) (DSPG)-contained lipid for delivery of purpurin 18 (MLP18) [44]. Due to the bacteria-oversecreted phospholipase A2 (PLA2) and maltodextrin transporter pathway, MLP18 achieved sonosensitizer targeted delivering by PLA2-mediated degradation and selectively be internalized into bacteria. The tissue NIR fluorescence and PA imaging results demonstrated MLP18 acted as a novel bacteria-targeted delivery system, which could precisely distinguish bacterial infections between sterile inflammation or cancer after via tail vein injection. Moreover, the MRI photographs in the MRSA-induced myositis model showed complete clearance of muscular lesions after MLP18-mediated SDT treatment.

5.5. Periodontal infection

Bacterial infection and biofilm formation are mainly caused by pulpal and periapical diseases [138]. Due to the unusual and complicated internal root canal, root canal treatment is a necessary and crucial clinical procedure for eliminating bacteria [139]. As the US serves as a common treatment tool and a non-invasive treatment in dentistry, Park et al. used a high-power US by creating vapor bubbles for root canal cleaning [140]. Dang et al. designed phase-change nanodroplets activated by the US that combined with 2 % chlorhexidine to remove *E. faecalis* biofilm in root canals [141]. As to avoid the use of an antibacterial agent, Guo et al. developed an M@P-Fe nanoplatform for root canal biofilm eradication based on SDT and chemodynamic therapy [54]. Compared to the Fenton reaction or SDT alone, combination therapy by M@P-Fe + 0.01 % H_2O_2 + US irradiation displayed a higher inhibition rate and more significant eradication efficacy biofilms in the root canals.

Periodontitis is a typical oral disease induced by periodontal bacterial infections, which affects more than 10 % of the global population [142]. Periodontitis not only causes periodontal tissue destruction and tooth loss but also associates with systemic diseases, including diabetes, atherosclerosis, etc. [143]. Xin et al. proposed TiO_2-grown mesoporous silica nanoparticles that doped Ag and modified with chitosan (DT-Ag-

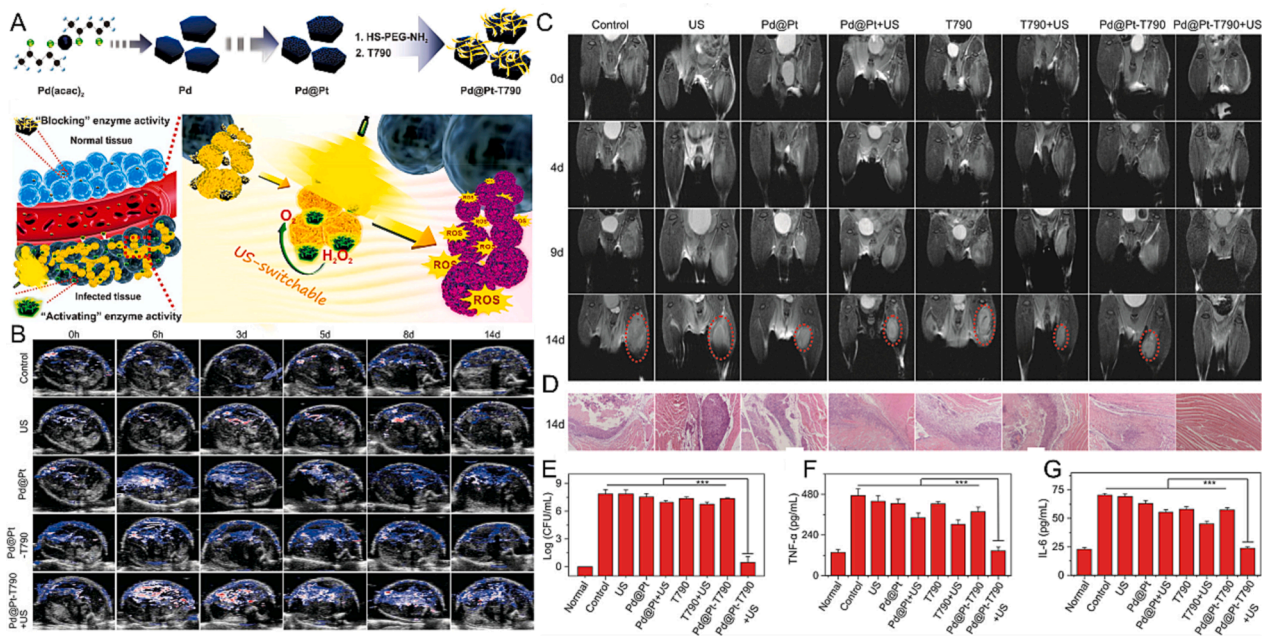

Fig. 8. Pd@Pt-T790 mediated SDT for myositis. (A) Schematic illustration of the main synthesis procedure of the Pd@Pt-T790 nanoplatform and its US-switchable nanozyme catalytic O_2-generation-enhanced SDT of bacterial infection. (B) Representative PA images of oxyhemoglobin saturation of the MRSA-infected mice within 14 days postinjection. (C) MRI images of the MRSA-infected mice. (D) H&E images of the MRSA myositis. (E) Quantitative results of bacterial culture from MRSA-infected leg tissues. (F) Serum TNF-α and (G) IL-6 levels of mice on day 14. Reproduced with permission [63].

CS^{+}) against *P. gingivalis*-induced periodontitis depending on chemodynamic-enhanced SDT [112]. Under H_2O_2 sufficient inflammatory microenvironment, Ag was found to act not only as generated •OH by catalyzing H_2O_2 but also as an antibacterial agent based on Ag^{+} releasement under US irradiation. The modification of quaternary ammonium chitosan was shown to improve the penetration into the bacterial outer membrane, thus substantially enhancing the anti-periodontitis efficacy *in vitro*. Compared with the untreated group, 3D CT images also demonstrated that the SDT combined with chemodynamic synergistic effect on inhibiting alveolar bone resorption, showing considerable potential for clinic applications in periodontitis.

5.6. Lung infection

Bacterial pneumonia is one of the most dangerous pulmonary diseases caused by various bacteria, resulting in acute and severe lung injury of humans [144]. The complex metabolic conditions of biofilm provided a physical barrier to reduce the therapeutic effect of antibacterial drugs in lung infection. Researchers found that SDT could improve drug diffusion in the targeted site and showed deeper penetration for enhanced therapeutic outcomes [145].

Xiu et al. designed piperacillin and Fe_3O_4 nanoparticles-loaded microbubbles (MB-Pip) based on self-assembly technology for *P. aeruginosa* biofilm-associated lung infection treatment [146]. In this platform, MB-Pip physically disrupted biofilms under US stimulation based on inertial cavitation, which subsequently enhanced the penetration of piperacillin and Fe_3O_4 nanoparticles into biofilms. Endogenous H_2O_2 in the infection site could be discomposed into ·OH for killing bacteria with the catalysis of Fe_3O_4 nanoparticles. In addition, Fe_3O_4 NPs could effectively activate antitumor immune responses for biofilm elimination by inducing M1-like macrophage polarization. This nanoplatform exhibited a noticeable enhancement of bacteria inhibition in infected lungs ($<10^2$ CFU/ml) *in vivo* compared to other groups. Both H&E, Masson, and Prussian blue staining of infected lung sections confirmed the SDT and chemotherapy synergistic effect of MB-Pip for *P. aeruginosa* biofilms destruction.

Pulmonary inhalation administration enabled the high local antibacterial concentration to locally treat lung infections [147]. Pan et al. utilized the ZIF-8-derived carbon@TiO_2 composites (ZTNs) as an inhalable nanosonosensitizer for the treatment of bacterial pneumonia (Fig. 9) [148]. ZTNs could be delivered into the pulmonary tract by aerosolized intratracheal inoculation and showed higher lung penetration depth under US irradiation. *In vitro* experiments, this nanoplatform showed efficient killing bacteria performance in the presence of US stimulation. The combination of SDT and inhalation administration *in vivo* showed great potential as an effective treatment strategy for bacterial pneumonia.

5.7. H. Pylori infection

H. pylori infection is the leading cause of gastrointestinal-based diseases, including gastric cancer, and has been influencing more than 50 % of the population worldwide [149]. SDT has exhibited potential in gastric infections treatment induced by *H. pylori* due to the ultra-high penetration depth of more than 10 cm. Wang et al. constructed HpAb-LiP-ICG nanoliposome to achieve US-activated *H. pylori* infection treatment. After oral administration, HpAb-LiP-ICG with specific targeting to the *H. pylori* membrane, and then produced $^1O_2$ to eliminate bacteria in the stomach [43]. In another study, Yu et al. reported a pH-responsive-based porphyrin MOF with peroxidase-like activity as anti-

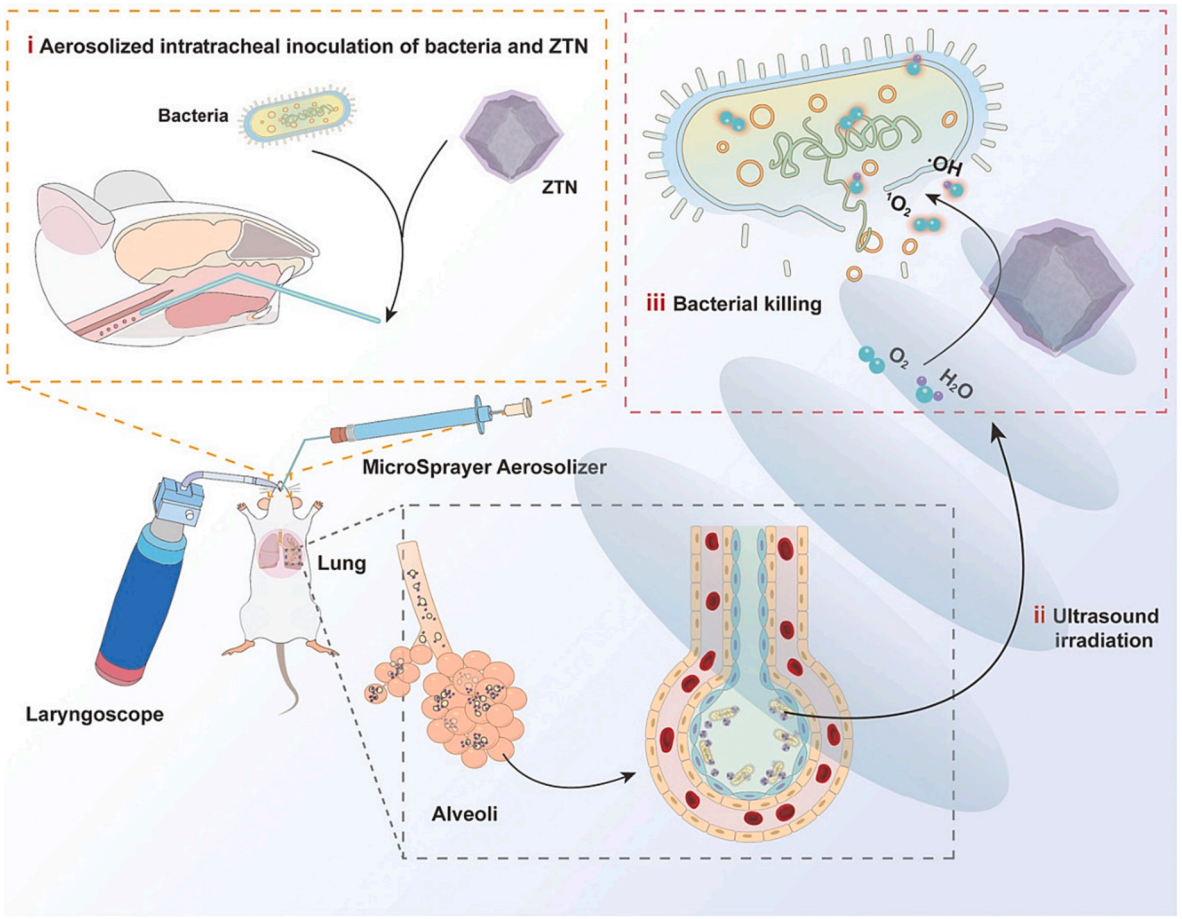

Fig. 9. Schematic illustration of ZTNs for SDT of bacterial lung infections. Reproduced with permission [148].

H. Pylori agents based on SDT and chemodynamic therapy [118]. In detail, these nanoplatform (Fe-HMME@DHA@MPN) were constructed by dihydroartemisinin loaded HMME/Fe(III) based MOF that surface modified with Fe (III)/tannic acid metal polyphenol network. *In vivo* experiments, the antibacterial efficiency was reached > 99.99 % against *H. pylori* strains even antibiotic-resistant *H. pylori* strains after combination treatment. The antibacterial ability *in vitro* demonstrated the combination of chemodynamic therapy and SDT anti-*H. Pylori* therapy showed similar therapeutic efficacy compared with antibiotic-based triple therapy. More importantly, the microbiome analysis of intestinal flora results demonstrated that the US treatment has minimal impact on gut microbiota, which may avoid the deterioration of homeostasis of intestinal flora caused by conventional triple therapy.

6. Conclusion and perspectives

In conclusion, the combination of nanomedicine and US-activated therapy holds a desirable prospect in biomedical applications. In this review, we have explicitly summarized the different classes of antibacterial nanoplatform for US-activated therapy in the past decade. Many types of nanoplatform were used for organic sonosensitizer delivery, such as liposome, polymer, MSN, and so on, which killed the bacterial cells and promoted bacteria-induced infection. In addition, nanoparticle-based sonosensitizer with multifunctionalities has been demonstrated as a feasible approach for antibacterial treatment. Along with these advances, US-activated antibacterial therapy in clinical bacteria-related infections management, such as skin infections, osteomyelitis, implant infections, myositis, periodontal infection, lung infection, and *H. pylori* infection diseases, have been summarized and discussed. Although extensive work has been devoted to the antibacterial application of nanoplatform with outstanding SDT performance, US-activated antibacterial therapy still faced some important challenges that must be bridged in the clinical translation.

(1) Benefiting from the deep tissue-penetrating capability (<1 cm) of US, SDT showed higher feasibility and better therapeutic efficiency compared with other antimicrobial therapies in deep tissue infections, such as osteomyelitis and myositis. However, the SDT equipment that adopted in past studies was relied on the available US processing device or assembled instruments based on a transducer and US probe. The US parameter could not be accurately and conveniently adjusted in those instruments, which may not meet the requirement of SDT process. Moreover, the cytotoxicity of SDT depend on different parameters *in vitro*, such as the thickness of coupling agent, the microplate size and the volume of bacteria medium. Thus, the novel US instrument that suitable for SDT application should be explored deeply and the US parameters in SDT-based antibacterial process should be standardized. With the devolvement of SDT equipment and standardized US parameters, the bottleneck of SDT based antibacterial application could be overcame.

(2) Combining novel nanomaterials and US techniques produces excellent antibacterial effects. The internal relationship between the US-activated SDT and bacteria must still be interpreted clearly. In addition to the fundamental mechanisms of SDT, the specific mechanisms of SDT towards different kinds of bacteria must be deeply excavated. In addition, ensuring the safety of normal tissues is as important as enhancing the antibacterial efficacy of nanomedicines in treatment. Thus, the therapeutic effect of US on pathogens and side effects on normal different tissue sites require to be continuously explored.

(3) The unsatisfied antibacterial efficacy of US-activated therapy demands novel design strategies of nanomedicines for achieving synergic treatment. Compared to monotherapy, combining US-activated therapy and other strategies, including chemotherapy, PTT, chemodynamic therapy, and gas therapy, could achieve a more efficient treatment outcome against pathogens via different pathways. Specifically, US-activated therapy-induced dead bacteria may awake the immune cells, and some nanoplatform also could activate the immune responses. In the future, more therapies could be integrated with US-activated therapy to achieve better antibacterial and antibiofilm effects.

(4) Despite US-activated nanosystems providing a potential strategy for bacterial eradication and biofilm elimination, the monitoring of the bacterial condition in infection site and treatment progress have gained remarkable attention. US technique also provides high sensitivity and excellent spatial resolution in imaging, which plays a significant role in medical fields. Therefore, we need to focus on the design of multifunctional nanosystems based on a US-activated strategy for the bacterial theranostics.

(5) The complicated infection microenvironment with acidic and hypoxic characteristics limits the further therapeutic performance of US-activated therapy. The design of nanotherapeutic agents with infection microenvironment-responsive properties, or targeting bacteria activity, is a meaningful research direction in the realm of US-activated targeting antibacterial therapy.

(6) The clinical translation of SDT for antibacterial application is still at the infant stage. Although the clearance pathway of many organic small-molecule sonosensitizers was clear, the clearance routes of nanoplatform loaded with organic sonosensitizers might change due to the particle size, shape, and composition of those nanoplatforms. Moreover, the nano-sonosensitizers could be cleared by renal, hepatobiliary, or mononuclear phagocytic system pathways. Current research has focused on the toxicity of nano-sonosensitizers *in vitro* experiments and mouse or rat models. The long-term safety and side effects of nano-sonosensitizers on different organs should be studied in more animal models.

To sum up, nanomedicine-enabled US-activated therapy has contributed substantially to bacterial-related infection fields. The prominent tissue penetration ability of the US ensures their deeper therapeutic depth and fewer side effects. Although it encourages the therapeutic performance of US-activated treatments, some crucial issues still remain and need to be solved in the field of SDT-based nanomedicine. We believe that with the sustained exploration of the mechanism of US-activated antibacterial therapy and innovation of nano biomaterials, US-activated therapy will act as a powerful weapon to fight against bacterial infections and will be gradually applied clinically in the near future.

CRediT authorship contribution statement

Pei-Yao Xu: Writing – original draft. **Ranjith Kumar Kankala:** Writing – original draft. **Shi-Bin Wang:** Writing – review & editing, Funding acquisition. **Ai-Zheng Chen:** Writing – review & editing, Funding acquisition.

Declaration of Competing Interest

The authors declare that they have no known competing financial interests or personal relationships that could have appeared to influence the work reported in this paper.

Data availability

Data will be made available on request.

Acknowledgments

Funding: This research was supported by the National Key Research & Development Program of China [grant number:2019YFE0113600],

the National Natural Science Foundation of China (NSFC) [grant number:81971734, 32071323, 32271410], the Science and Technology Projects in Fujian Province [grant number:2022FX1, 2023Y4008], and Program for Innovative Research Team in Science, Scientific Research Funds of Huaqiao University [grant number:21BS113].

References

[1] C. Deusenbery, Y.Y. Wang, A. Shukla, Recent innovations in bacterial infection detection and treatment, ACS Infect. Dis. 7 (2021) 695–720, https://doi.org/10.1021/acsinfecdis.0c00890.
[2] P. Beyer, S. Paulin, The antibacterial research and development pipeline needs urgent solutions, ACS Infect. Dis. 6 (2020) 1289–1291, https://doi.org/10.1021/acsinfecdis.0c00044.
[3] R. Canaparo, F. Foglietta, N. Barbero, L. Serpe, The promising interplay between sonodynamic therapy and nanomedicine, Adv. Drug Deliv. Rev. 189 (2022), 114495, https://doi.org/10.1016/j.addr.2022.114495.
[4] O. Ciofu, C. Moser, P.O. Jensen, N. Hoiby, Tolerance and resistance of microbial biofilms, Nat. Rev. Microbiol. 20 (2022) 621–635, https://doi.org/10.1038/s41579-022-00682-4.
[5] G.J. Mi, D. Shi, M. Wang, T.J. Webster, Reducing bacterial infections and biofilm formation using nanoparticles and nanostructured antibacterial surfaces, Adv. Healthc. Mater. 7 (2018) 1800103, https://doi.org/10.1002/adhm.201800103.
[6] B.M. Bakadia, L. Lamboni, A.A. Qaed Ahmed, R. Zheng, B.O. Ode Boni, Z. Shi, S. Song, T. Souho, B.M. Mukole, F. Qi, G. Yang, Antibacterial silk sericin/poly (vinyl alcohol) hydrogel with antifungal property for potential infected large burn wound healing: systemic evaluation, Smart Mater. Med. 4 (2023) 37–58, https://doi.org/10.1016/j.smaim.2022.07.002.
[7] M.J. Xu, L. Li, Q.L. Hu, The recent progress in photothermal-triggered bacterial eradication, Biomater. Sci. 9 (2021) 1995–2008, https://doi.org/10.1039/d0bm02057e.
[8] J. Huo, Q. Jia, H. Huang, J. Zhang, P. Li, X. Dong, W. Huang, Emerging photothermal-derived multimodal synergistic therapy in combating bacterial infections, Chem. Soc. Rev. 50 (2021) 8762–8789, https://doi.org/10.1039/D1CS00074H.
[9] Y.F. Feng, C.C. Tonon, S. Ashraf, T. Hasan, Photodynamic and antibiotic therapy in combination against bacterial infections: efficacy, determinants, mechanisms, and future perspectives, Adv. Drug Deliv. Rev. 177 (2021), 113941, https://doi.org/10.1016/j.addr.2021.113941.
[10] R.H. Wang, Q.W. Liu, A. Gao, N. Tang, Q. Zhang, A.M. Zhang, D.X. Cui, Recent developments of sonodynamic therapy in antibacterial application, Nanoscale 14 (2022) 12999–13017, https://doi.org/10.1039/d2nr01847k.
[11] X. Pang, D.F. Li, J. Zhu, J.L. Cheng, G. Liu, Beyond antibiotics: Photo/sonodynamic approaches for bacterial theranostics, Nano-Micro Lett. 12 (2020) 23, https://doi.org/10.1007/s40820-020-00485-3.
[12] Q.L. Guo, X.L. Dai, M.Y. Yin, H.W. Cheng, H.S. Qian, H. Wang, D.M. Zhu, X. W. Wang, Nanosensitizers for sonodynamic therapy for glioblastoma multiforme: current progress and future perspectives, Mil. Med. Res. 9 (2022) 18, https://doi.org/10.1186/s40779-022-00386-z.
[13] Q.L. Xu, W.J. Xiu, Q. Li, Y. Zhang, X.Y. Li, M. Ding, D.L. Yang, Y.B. Mou, H. Dong, Emerging nanosonosensitizers augment sonodynamic-mediated antimicrobial therapies, Mater. Today Bio 19 (2023), 100559, https://doi.org/10.1016/j.mtbio.2023.100559.
[14] H.A. Hemeg, Nanomaterials for alternative antibacterial therapy, Int. J. Nanomed. 12 (2017) 8211–8225, https://doi.org/10.2147/ijn.s132163.
[15] P.Y. Xu, R.K. Kankala, Y.W. Li, S.B. Wang, A.Z. Chen, Synergistic chemo-/photothermal therapy based on supercritical technology-assisted chitosan-indocyanine green/luteolin nanocomposites for wound healing, Regen. Biomater. 9 (2022) rbac072, https://doi.org/10.1093/rb/rbac072.
[16] B.Q. Chen, Y. Zhao, Y. Zhang, Y.J. Pan, H.Y. Xia, R.K. Kankala, S.B. Wang, G. Liu, A.Z. Chen, Immune-regulating camouflaged nanoplatforms: a promising strategy to improve cancer nano-immunotherapy, Bioact. Mater. 21 (2023) 1–19, https://doi.org/10.1016/j.bioactmat.2022.07.023.
[17] T. Xu, S.J. Zhao, C.W. Lin, X.L. Zheng, M.H. Lan, Recent advances in nanomaterials for sonodynamic therapy, Nano Res. 13 (2020) 2898–2908, https://doi.org/10.1007/s12274-020-2992-5.
[18] A. Harada, M. Ono, E. Yuba, K. Kono, Titanium dioxide nanoparticle-entrapped polyion complex micelles generate singlet oxygen in the cells by ultrasound irradiation for sonodynamic therapy, Biomater. Sci. 1 (2013) 65–73, https://doi.org/10.1039/c2bm00066k.
[19] X. Wang, X. Wang, Q. Yue, H. Xu, X. Zhong, L. Sun, G. Li, Y. Gong, N. Yang, Z. Wang, Z. Liu, L. Cheng, Liquid exfoliation of TiN nanodots as novel sonosensitizers for photothermal-enhanced sonodynamic therapy against cancer, Nano Today 39 (2021), 101170, https://doi.org/10.1016/j.nantod.2021.101170.
[20] Z. He, J. Du, Y. Miao, Y. Li, Recent developments of inorganic nanosensitizers for sonodynamic therapy, Adv. Healthc. Mater. 12 (2023), 2300234, https://doi.org/10.1002/adhm.202300234.
[21] J. Ouyang, Z.M. Tang, N. Farokhzad, N. Kong, N.Y. Kim, C. Feng, S. Blake, Y. F. Xiao, C. Liu, T. Xie, W. Tao, Ultrasound mediated therapy: Recent progress and challenges in nanoscience, Nano Today 35 (2020), 100949, https://doi.org/10.1016/j.nantod.2020.100949.
[22] F.F. Yang, J. Dong, Z.F. Li, Z.H. Wang, Metal-organic frameworks (MOF)-assisted sonodynamic therapy in anticancer applications, ACS Nano 17 (2023) 4102–4133, https://doi.org/10.1021/acsnano.2c10251.
[23] I. Rosenthal, J.Z. Sostaric, P. Riesz, Sonodynamic therapy - a review of the synergistic effects of drugs and ultrasound, Ultrason. Sonochem. 11 (2004) 349–363, https://doi.org/10.1016/j.ultsonch.2004.03.004.
[24] X.S. Cao, M.X. Li, Q.Y. Liu, J.J. Zhao, X.H. Lu, J.W. Wang, Inorganic sonosensitizers for sonodynamic therapy in cancer treatment, Small (2023), 2303195, https://doi.org/10.1002/smll.202303195.
[25] Y.R. Yang, J. Huang, M. Liu, Y.G. Qiu, Q.H. Chen, T.J. Zhao, Z.X. Xiao, Y.Q. Yang, Y.T. Jiang, Q. Huang, K.L. Ai, Emerging sonodynamic therapy-based nanomedicines for cancer immunotherapy, Adv. Sci. 10 (2023), 2204365, https://doi.org/10.1002/advs.202204365.
[26] G. Canavese, A. Ancona, L. Racca, M. Canta, B. Dumontel, F. Barbaresco, T. Limongi, V. Cauda, Nanoparticle-assisted ultrasound: A special focus on sonodynamic therapy against cancer, Chem. Eng. J. 340 (2018) 155–172, https://doi.org/10.1016/j.cej.2018.01.060.
[27] X. Xing, S. Zhao, T. Xu, L. Huang, Y. Zhang, M. Lan, C. Lin, X. Zheng, P. Wang, Advances and perspectives in organic sonosensitizers for sonodynamic therapy, Coord. Chem. Rev. 445 (2021), 214087, https://doi.org/10.1016/j.ccr.2021.214087.
[28] V.B. Borisov, S.A. Siletsky, M.R. Nastasi, E. Forte, ROS defense systems and terminal oxidases in bacteria, Antioxidants 10 (2021) 839, https://doi.org/10.3390/antiox10060839.
[29] C.M. Runyan, J.C. Carmen, B.L. Beckstead, J.L. Nelson, R.A. Robison, W.G. Pitt, Low-frequency ultrasound increases outer membrane permeability of Pseudomonas aeruginosa, J. Gen. Appl. Microbiol. 52 (2006) 295–301, https://doi.org/10.2323/jgam.52.295.
[30] F. Nakonechny, M. Nisnevitch, Different aspects of using ultrasound to combat microorganisms, Adv. Funct. Mater. 31 (2021) 2011042, https://doi.org/10.1002/adfm.202011042.
[31] P. Liu, T.Y. Yang, Y.N. Li, J. Guo, S.L. Li, H.L. Chen, Y. Liu, Nanomaterial-based sonosensitizers: from exemplary design towards purposeful improvement, Mat. Chem. Front. 7 (2023) 985–1003, https://doi.org/10.1039/d2qm01267g.
[32] X. Song, Q. Zhang, M. Chang, L. Ding, H. Huang, W. Feng, T. Xu, Y. Chen, Nanomedicine-enabled sonomechanical, sonopiezoelectric, sonodynamic and sonothermal therapy, Adv. Mater. (2023) e2212259.
[33] J. Cao, M.X. Zheng, Z.Y. Sun, Z.Y. Li, X.Y. Qi, S. Shen, One-step fabrication of multifunctional PLGA-HMME-DTX@MnO2 nanoparticles for enhanced chemo-sonodynamic antitumor treatment, Int. J. Nanomed. 17 (2022) 2577–2591, https://doi.org/10.2147/ijn.s365570.
[34] T.G.N. Cao, Q.T. Hoang, E.J. Hong, S.J. Kang, J.H. Kang, V. Ravichandran, H. C. Kang, Y.T. Ko, W.J. Rhee, M.S. Shim, Mitochondria-targeting sonosensitizer-loaded extracellular vesicles for chemo-sonodynamic therapy, J. Control. Release 354 (2023) 651–663, https://doi.org/10.1016/j.jconrel.2023.01.044.
[35] L.S. Zhu, Y. Yang, X.D. Li, Y.L. Zheng, Z.Y. Li, H.J. Chen, Y. Gao, Facile preparation of indocyanine green and tiny gold nanoclusters co-loaded nanocapsules for targeted synergistic sono-/photo-therapy, J. Colloid Interface Sci. 627 (2022) 596–609, https://doi.org/10.1016/j.jcis.2022.07.084.
[36] P.Y. Xu, X. Zheng, R.K. Kankala, S.B. Wang, A.Z. Chen, Advances in indocyanine green-based codelivery nanoplatforms for combinatorial therapy, ACS Biomater Sci. Eng. 7 (2021) 939–962, https://doi.org/10.1021/acsbiomaterials.0c01644.
[37] Y. Tian, Y. Liu, L.K. Wang, X.Y. Guo, Y.P. Liu, J. Mou, H.X. Wu, S.P. Yang, Gadolinium-doped hollow silica nanospheres loaded with curcumin for magnetic resonance imaging-guided synergistic cancer sonodynamic-chemotherapy, Mater. Sci. Eng., C, 126 (2021) 112157. 10.1016/j.msec.2021.112157.
[38] L.F. Chen, P.Y. Xu, S.B. Wang, A.Z. Chen, Research progress of tumor sonodynamic therapy based on nanomaterials, Chin. Sci. Bull. 66 (2021) 1057–1066, https://doi.org/10.1360/tb-2020-1053.
[39] D.G. Zhang, B.Q. Chen, Y.J. Pan, H. Liu, Y.H. Shi, L.F. Chen, R.K. Kankala, S. B. Wang, A.Z. Chen, Albumin-based smart nanoplatform for ultrasound-mediated enhanced chemo-sonodynamic combination therapy, Mater. Des. 227 (2023), 111794, https://doi.org/10.1016/j.matdes.2023.111794.
[40] F. Raza, L. Evans, M. Motallebi, H. Zafar, M. Pereira-Silva, K. Saleem, D. Peixoto, A. Rahdar, E. Sharifi, F. Veiga, C. Hoskins, A.C. Paiva-Santos, Liposome-based diagnostic and therapeutic applications for pancreatic cancer, Acta Biomater. 157 (2023) 1–23, https://doi.org/10.1016/j.actbio.2022.12.013.
[41] V. De Leo, A.M. Maurelli, L. Giotta, L. Catucci, Liposomes containing nanoparticles: preparation and applications, Colloids Surf. B 218 (2022), 112737, https://doi.org/10.1016/j.colsurfb.2022.112737.
[42] M. Pourhajibagher, B. Rahimi-esboei, H. Ahmadi, A. Bahador, The anti-biofilm capability of nano-emodin-mediated sonodynamic therapy on multi-species biofilms produced by burn wound bacterial strains, Photodiagn. Photodyn. Ther. 34 (2021), 102288, https://doi.org/10.1016/j.pdpdt.2021.102288.
[43] R.H. Wang, C.F. Song, A. Gao, Q.W. Liu, W.B. Guan, J.W. Mei, L.J. Ma, D.X. Cui, Antibody-conjugated liposomes loaded with indocyanine green for oral targeted photoacoustic imaging-guided sonodynamic therapy of Helicobacter pylori infection, Acta Biomater. 143 (2022) 418–427, https://doi.org/10.1016/j.actbio.2022.02.031.
[44] X. Pang, Q.C. Xiao, Y. Cheng, E. Ren, L.L. Lian, Y. Zhang, H.Y. Gao, X.Y. Wang, W. N. Leung, X.Y. Chen, G. Liu, C.S. Xu, Bacteria-responsive nanoliposomes as smart sonotheranostics for multidrug resistant bacterial infections, ACS Nano 13 (2019) 2427–2438, https://doi.org/10.1021/acsnano.8b09336.
[45] R. Zhang, L. Zhang, H.T. Ran, P. Li, J. Huang, M.X. Tan, Y. Yang, Z.G. Wang, A mitochondria-targeted anticancer nanoplatform with deep penetration for enhanced synergistic sonodynamic and starvation therapy, Biomater. Sci. 8 (2020) 4581–4594, https://doi.org/10.1039/d0bm00408a.
[46] J. Kopecek, J.Y. Yang, Polymer nanomedicines, Adv. Drug Deliv. Rev. 156 (2020) 40–64, https://doi.org/10.1016/j.addr.2020.07.020.

[47] Y. Su, C. Wang, H. Zhang, L.F. Guo, Y.S. Liang, M. Xiong, X.H. Feng, D.S. Chen, Z. Y. Ke, L. Wen, G. Chen, Sonodynamic therapy exciting the herbal nanocomposite with spider-web-like effect to combat otitis media, Int. J. Pharm. 621 (2022), 121820, https://doi.org/10.1016/j.ijpharm.2022.121820.
[48] A. Aldegheishem, R. Alharthi, Y.M. Al-Qahtani, M. Soliman, M.S. Mostafa, S. F. Mohsin, E. Eldwakhly, Mechanical and antibacterial efficacy of photo-sonodynamic therapy via methylene blue-loaded nanoparticles over dental implants for treating peri-implantitis, Photodiagn. Photodyn. Ther. 40 (2022), 103188, https://doi.org/10.1016/j.pdpdt.2022.103188.
[49] S.J. Chen, J.H. Wang, K. Tang, H.Q. Liao, Y. Xu, L. Wang, C.C. Niu, Multi-modal imaging monitored M2 macrophage targeting sono-responsive nanoparticles to combat MRSA deep infections, Int. J. Nanomed. 17 (2022) 4525–4546, https://doi.org/10.2147/ijn.S383237.
[50] M. Pourhajibagher, B.R. Esboei, M. Hodjat, A. Bahador, Sonodynamic excitation of nanomicelle curcumin for eradication of Streptococcus mutans under sonodynamic antimicrobial chemotherapy: enhanced anti-caries activity of nanomicelle curcumin, Photodiagn. Photodyn. Ther. 30 (2020), 101780, https://doi.org/10.1016/j.pdpdt.2020.101780.
[51] D. Wang, D.B. Cheng, L. Ji, L.J. Niu, X.H. Zhang, Y. Cong, R.H. Cao, L. Zhou, F. Bai, Z.Y. Qiao, H. Wang, Precise magnetic resonance imaging-guided sonodynamic therapy for drug-resistant bacterial deep infection, Biomaterials 264 (2021), 120386, https://doi.org/10.1016/j.biomaterials.2020.120386.
[52] W. Li, Y. Jiang, J. Lu, Nanotechnology-enabled immunogenic cell death for improved cancer immunotherapy, Int. J. Pharm. 634 (2023), 122655, https://doi.org/10.1016/j.ijpharm.2023.122655.
[53] R.K. Kankala, H.B. Zhang, C.G. Liu, K.R. Kanubaddi, C.H. Lee, S.B. Wang, W. G. Cui, H.A. Santos, K.L. Lin, A.Z. Chen, Metal species-encapsulated mesoporous silica nanoparticles: Current advancements and latest breakthroughs, Adv. Funct. Mater. 29 (2019), 1902652, https://doi.org/10.1002/adfm.201902652.
[54] J.M. Guo, Y. Xu, M.D. Liu, J. Yu, H.Y. Yang, W.L. Lei, C. Huang, An MSN-based synergistic nanoplatform for root canal biofilm eradication via Fenton-enhanced sonodynamic therapy, J. Mat. Chem. B 9 (2021) 7686–7697, https://doi.org/10.1039/d1tb01031j.
[55] Y.M. Zhao, M. Hu, Y.F. Zhang, J.H. Liu, C.C. Liu, S.K. Choi, Z.X. Zhang, L.Q. Song, Multifunctional therapeutic strategy of Ag-synergized dual-modality upconversion nanoparticles to achieve the rapid and sustained cidality of methicillin-resistant Staphylococcus aureus, Chem. Eng. J. 385 (2020), 123980, https://doi.org/10.1016/j.cej.2019.123980.
[56] H.P. Liu, J.F. Li, X.M. Liu, Z.Y. Li, Y. Zhang, Y.Q. Liang, Y.F. Zheng, S.L. Zhu, Z. D. Cui, S.L. Wu, Photo-sono interfacial engineering exciting the intrinsic rroperty of herbal nanomedicine for rapid broad-spectrum bacteria killing, ACS Nano 15 (2021) 18505–18519, https://doi.org/10.1021/acsnano.1c08409.
[57] W. Huang, B. Hu, Y. Yuan, H. Fang, J. Jiang, Q. Li, Y. Zhuo, X. Yang, J. Wei, X. Wang, Visible light-responsive selenium nanoparticles combined with sonodynamic therapy to promote wound healing, ACS Biomater Sci. Eng. 9 (2023) 1341–1351, https://doi.org/10.1021/acsbiomaterials.2c01119.
[58] H. Dong, W.J. Xiu, L. Wan, Q. Li, Y. Zhang, M. Ding, J.Y. Shan, K.L. Yang, Z. G. Teng, L.H. Yuwen, Y.B. Mou, Biofilm microenvironment response nanoplatform synergistically degrades biofilm structure and relieves hypoxia for efficient sonodynamic therapy, Chem. Eng. J. 453 (2023), 139839, https://doi.org/10.1016/j.cej.2022.139839.
[59] X. Sun, M.S. Wei, X. Pang, L. Lin, Q. Gao, L.C. Su, T. Liu, Y.L. Yao, J.B. Song, W. Wang, X.H. Yan, Sonodynamic bacterial inactivation enhanced by an actuator-integrated mechanism, Adv. Funct. Mater. (2023) 2214619, https://doi.org/10.1002/adfm.202214619.
[60] X.R. Geng, Y.H. Chen, Z.Y. Chen, X.Y. Wei, Y.L. Dai, Z. Yuan, Oxygen-carrying biomimetic nanoplatform for sonodynamic killing of bacteria and treatment of infection diseases, Ultrason. Sonochem. 84 (2022), 105972, https://doi.org/10.1016/j.ultsonch.2022.105972.
[61] H. Lin, C. Yang, Y. Luo, M. Ge, H. Shen, X.L. Zhang, J.L. Shi, Biomimetic nanomedicine-triggered in situ vaccination for innate and adaptive immunity activations for bacterial osteomyelitis treatment, ACS Nano 16 (2022) 5943–5960, https://doi.org/10.1021/acsnano.1c11132.
[62] B. Huang, L. Wang, K. Tang, S. Chen, Y. Xu, H. Liao, C. Niu, IR780 based sonotherapeutic nanoparticles to combat multidrug-resistant bacterial infections, Front. Chem. 10 (2022), 840598, https://doi.org/10.3389/fchem.2022.840598.
[63] D. Sun, X. Pang, Y. Cheng, J. Ming, S. Xiang, C. Zhang, P. Lv, C. Chu, X. Chen, G. Liu, N. Zheng, Ultrasound-switchable nanozyme augments sonodynamic therapy against multidrug-resistant bacterial infection, ACS Nano 14 (2020) 2063–2076, https://doi.org/10.1021/acsnano.9b08667.
[64] Y.Q. Yang, X.W. Wang, H.S. Qian, L. Cheng, Titanium-based sonosensitizers for sonodynamic cancer therapy, Appl. Mater. Today 25 (2021), 101215, https://doi.org/10.1016/j.apmt.2021.101215.
[65] X. Wang, X. Zhong, L. Bai, J. Xu, F. Gong, Z. Dong, Z. Yang, Z. Zeng, Z. Liu, L. Cheng, Ultrafine titanium monoxide (TiO1+x) nanorods for enhanced sonodynamic therapy, J. Am. Chem. Soc. 142 (2020) 6527–6537, https://doi.org/10.1021/jacs.9b10228.
[66] W.H. Guo, T. Wang, C.Y. Huang, S.P. Ning, Q.L. Guo, W. Zhang, H.W. Yang, D. M. Zhu, Q.Q. Huang, H.S. Qian, X.W. Wang, Platelet membrane-coated C-TiO2 hollow nanospheres for combined sonodynamic and alkyl-radical cancer therapy, Nano Res. 16 (2023) 782–791, https://doi.org/10.1007/s12274-022-4646-2.
[67] S. Ning, X. Dai, W. Tang, Q. Guo, M. Lyu, D. Zhu, W. Zhang, H. Qian, X. Yao, X. Wang, Cancer cell membrane-coated C-TiO2 hollow nanoshells for combined sonodynamic and hypoxia-activated chemotherapy, Acta Biomater. 152 (2022) 562–574, https://doi.org/10.1016/j.actbio.2022.08.067.
[68] Q.L. Ouyang, Y.X. Zeng, Y. Yu, L. Tan, X.M. Liu, Y.F. Zheng, S.L. Wu, Ultrasound-responsive microneedles eradicate deep-layered wound biofilm based on TiO2 crystal phase engineering, Small 19 (2023), 2205292, https://doi.org/10.1002/smll.202205292.
[69] Y.Q. Zhu, W.Q. Huang, G. Chen, L. Xia, Y.Z. You, Y. Yu, Sticking-bacteria gel enhancing anti-multidrug-resistant microbial therapy under ultrasound, Nano Res. 15 (2022) 9105–9113, https://doi.org/10.1007/s12274-022-4547-4.
[70] X.W. Wang, X.Y. Zhong, L. Cheng, Titanium-based nanomaterials for cancer theranostics, Coord. Chem. Rev. 430 (2021), 213662, https://doi.org/10.1016/j.ccr.2020.213662.
[71] K. Su, L. Tan, X.M. Liu, Z.D. Cui, Y.F. Zheng, B. Li, Y. Han, Z.Y. Li, S.L. Zhu, Y. Q. Liang, X.B. Feng, X.B. Wang, S.L. Wu, Rapid Photo-Sonotherapy for clinical treatment of bacterial Infected bone implants by creating oxygen deficiency Using Sulfur Doping, ACS Nano 14 (2020) 2077–2089, https://doi.org/10.1021/acsnano.9b08686.
[72] M. Liang, L. Shang, Y. Yu, Y. Jiang, Q. Bai, J. Ma, D. Yang, N. Sui, Z. Zhu, Ultrasound activatable microneedles for bilaterally augmented sono-chemodynamic and sonothermal antibacterial therapy, Acta Biomater. 158 (2022) 811–826, https://doi.org/10.1016/j.actbio.2022.12.041.
[73] Y. Sun, W.Z. Xu, C. Jiang, T.Y. Zhou, Q.Q. Wang, A. Lan, Gold nanoparticle decoration potentiate the antibacterial enhancement of TiO2 nanotubes via sonodynamic therapy against peri-implant infections, Front. Bioeng. Biotechnol. 10 (2022), 1074083, https://doi.org/10.3389/fbioe.2022.1074083.
[74] S. Cheng, M.L. Qi, W. Li, W.Y. Sun, M.Q. Li, J.Y. Lin, X. Bai, Y. Sun, B. Dong, L. Wang, Dual-responsive nanocomposites for synergistic antibacterial therapies facilitating bacteria-infected wound healing, Adv. Healthc. Mater. 12 (2022), 2202652, https://doi.org/10.1002/adhm.202202652.
[75] P. Wang, Q.S. Tang, L.L. Zhang, M.H. Xu, L.H. Sun, S.H. Sun, J.X. Zhang, S. M. Wang, X.L. Liang, Ultrasmall barium titanate nanoparticles for highly efficient hypoxic tumor therapy via ultrasound triggered piezocatalysis and water splitting, ACS Nano 15 (2021) 11326–11340, https://doi.org/10.1021/acsnano.1c00616.
[76] D. Liu, L. Li, B.L. Shi, B. Shi, M.D. Li, Y. Qiu, D. Zhao, Q.D. Shen, Z.Z. Zhu, Ultrasound-triggered piezocatalytic composite hydrogels for promoting bacterial-infected wound healing, Bioact. Mater. 24 (2023) 96–111, https://doi.org/10.1016/j.bioactmat.2022.11.023.
[77] Z. Zhu, X. Gou, L. Liu, T. Xia, J. Wang, Y. Zhang, C. Huang, W. Zhi, R. Wang, X. Li, S. Luo, Dynamically evolving piezoelectric nanocomposites for antibacterial and repair-promoting applications in infected wound healing, Acta Biomater. 157 (2023) 566–577, https://doi.org/10.1016/j.actbio.2022.11.061.
[78] D. He, W. Wang, N. Feng, Z. Zhang, D. Zhou, J. Zhang, H. Luo, Y. Li, X. Chen, J. Wu, Defect-modified nano-BaTiO3 as a sonosensitizer for rapid and high-efficiency sonodynamic sterilization, ACS Appl. Mater. Interfaces 15 (2023) 15140–15151, https://doi.org/10.1021/acsami.2c23113.
[79] J. Lei, C.F. Wang, X.B. Feng, L. Ma, X.M. Liu, Y. Luo, L. Tan, S.L. Wu, C. Yang, Sulfur-regulated defect engineering for enhanced ultrasonic piezocatalytic therapy of bacteria-infected bone defects, Chem. Eng. J. 435 (2022), 134624, https://doi.org/10.1016/j.cej.2022.134624.
[80] M.Q. Wu, Z.Y. Zhang, Z.R. Liu, J.M. Zhang, Y.L. Zhang, Y.M. Ding, T. Huang, D. L. Xiang, Z. Wang, Y.J. Dai, X.Y. Wan, S.B. Wang, H.L. Qian, Q.J. Sun, L.L. Li, Piezoelectric nanocomposites for sonodynamic bacterial elimination and wound healing, Nano Today 37 (2021), 101104, https://doi.org/10.1016/j.nantod.2021.101104.
[81] Q. Gao, Z. Wang, Y. Rao, Y. Zhao, J. Cao, K.-F. Ho, Y. Zhai, M. Xiong, J. Li, Y. Huang, Oxygen vacancy mediated α-MoO3 bactericidal nanocatalyst in the dark: Surface structure dependent superoxide generation and antibacterial mechanisms, J. Hazard. Mater. 443 (2023), 130275, https://doi.org/10.1016/j.jhazmat.2022.130275.
[82] H.Z. Chen, X.J. He, Z. Zhou, Z.K. Wu, H. Li, X.S. Peng, Y.B. Zhou, C.L. Tan, J. L. Shen, Metallic phase enabling MoS2 nanosheets as an efficient sonosensitizer for photothermal-enhanced sonodynamic antibacterial therapy, J. Nanobiotechnol. 20 (2022) 136, https://doi.org/10.1186/s12951-022-01344-6.
[83] X. Feng, J. Lei, L. Ma, Q. Ouyang, Y. Zeng, H. Liang, C. Lei, G. Li, L. Tan, X. Liu, C. Yang, Ultrasonic interfacial engineering of MoS2-modified Zn single-atom catalysts for efficient osteomyelitis sonodynamic ion therapy, Small 18 (2022), 2105775, https://doi.org/10.1002/smll.202105775.
[84] X. Gao, Y. Liu, Y. Li, B. Jin, P. Jiang, X. Chen, C. Wei, J. Sheng, Y.-N. Liu, J. Li, W. Chen, Piezoelectric nanozyme for dual-driven catalytic eradication of bacterial biofilms, ACS Appl. Mater. Interfaces 15 (2023) 14690–14703, https://doi.org/10.1021/acsami.2c21901.
[85] X.J. He, J.T. Hou, X.S. Sun, P. Jangili, J.S. An, Y.N. Qian, J.S. Kim, J.L. Shen, NIR-II photo-amplified sonodynamic therapy using sodium molybdenum bronze nanoplatform against subcutaneous staphylococcus aureus infection, Adv. Funct. Mater. 32 (2022), 2203964, https://doi.org/10.1002/adfm.202203964.
[86] L. Zong, Y. Yu, J. Wang, P. Liu, W. Feng, X. Dai, L. Chen, C. Gunawan, S.L. Jimmy Yun, R. Amal, S. Cheong, Z. Gu, Y. Chen, Oxygen-vacancy-rich molybdenum carbide MXene nanonetworks for ultrasound-triggered and capturing-enhanced sonocatalytic bacteria eradication, Biomaterials 296 (2023), 122074, https://doi.org/10.1016/j.biomaterials.2023.122074.
[87] F.C. Cui, T.T. Li, D.F. Wang, S.M. Yi, J.R. Li, X.P. Li, Recent advances in carbon-based nanomaterials for combating bacterial biofilm-associated infections, J. Hazard. Mater. 431 (2022), 128597, https://doi.org/10.1016/j.jhazmat.2022.128597.
[88] D. Liu, X. Dai, W. Zhang, X. Zhu, Z. Zha, H. Qian, L. Cheng, X. Wang, Liquid exfoliation of ultrasmall zirconium carbide nanodots as a noninflammatory

photothermal agent in the treatment of glioma, Biomaterials 292 (2023), 121917, https://doi.org/10.1016/j.biomaterials.2022.121917.
[89] G.Q. Li, X.Y. Zhong, X.W. Wang, F. Gong, H.L. Lei, Y.K. Zhou, C.F. Li, Z.D. Xiao, G. X. Ren, L. Zhang, Z.Q. Dong, Z. Liu, L. Cheng, Titanium carbide nanosheets with defect structure for photothermal-enhanced sonodynamic therapy, Bioact. Mater. 8 (2022) 409–419, https://doi.org/10.1016/j.bioactmat.2021.06.021.
[90] M.Y. Ku, C.Y. Mao, S.L. Wu, Y.F. Zheng, Z.Y. Li, Z.D. Cui, S.L. Zhu, J. Shen, X. M. Liu, Lattice strain engineering of Ti3C2 narrows band gap for realizing extraordinary sonocatalytic bacterial killing, ACS Nano 17 (2023) 14840–14851, https://doi.org/10.1021/acsnano.3c03134.
[91] C.Y. Mao, W.Y. Jin, Y.M. Xiang, Y.Z. Zhu, J. Wu, X.M. Liu, S.L. Wu, Y.F. Zheng, K. M.C. Cheung, K.W.K. Yeung, Realizing highly efficient sonodynamic bactericidal capability through the phonon-electron coupling effect using two-dimensional catalytic planar defects, Adv. Mater., 35 2208681. 10.1002/adma.202208681.
[92] Y. Yu, H.Y. Sun, Q.S. Lu, J.Y. Sun, P.F. Zhang, L.R. Zeng, K. Vasilev, Y.P. Zhao, Y. Chen, P.L. Liu, Spontaneous formation of MXene-oxidized sono/chemo-dynamic sonosensitizer/nanocatalyst for antibacteria and bone-tissue regeneration, J. Nanobiotechnol. 21 (2023) 21, https://doi.org/10.1186/s12951-023-01933-z.
[93] J. Li, X. Liu, Y. Zheng, Z. Cui, H. Jiang, Z. Li, S. Zhu, S. Wu, Achieving fast charge separation by ferroelectric ultrasonic interfacial engineering for rapid sonotherapy of bacteria-infected osteomyelitis, Adv. Mater. 35 (2023), 2210296, https://doi.org/10.1002/adma.202210296.
[94] Q. Bai, J.C. Zhang, Y.X. Yu, C.H. Zhang, Y.J. Jiang, D.Q. Yang, M.H. Liu, L. N. Wang, F.L. Du, N. Sui, Z.L. Zhu, Piezoelectric activatable nanozyme-based skin patch for rapid wound disinfection, ACS Appl. Mater. Interfaces 14 (2022) 26455–26468, https://doi.org/10.1021/acsami.2c05114.
[95] S. Shi, Y. Jiang, Y. Yu, M. Liang, Q. Bai, L. Wang, D. Yang, N. Sui, Z. Zhu, Piezo-augmented and photocatalytic nanozyme integrated microneedles for antibacterial and anti-Inflammatory combination therapy, Adv. Funct. Mater. 33 (2023), 2210850, https://doi.org/10.1002/adfm.202210850.
[96] C. Lu, Y. Tian, H. Tian, B. Li, B. Peng, J. Zheng, Y.L. Dai, An ultrasound activable metal-phenolic network nano-antibiotics for in vivo on-site infection therapy, Sci. China Mater. 66 (2023) 395–406, https://doi.org/10.1007/s40843-022-2125-1.
[97] X.L. Bi, Q. Bai, M.M. Liang, D.Q. Yang, S.H. Li, L.N. Wang, J. Liu, W.W. Yu, N. Sui, Z.L. Zhu, Silver peroxide nanoparticles for combined antibacterial sonodynamic and photothermal therapy, Small 18 (2022), 2104160, https://doi.org/10.1002/smll.202104160.
[98] S. Cheng, L. Chen, F. Gong, X. Yang, Z. Han, Y. Wang, J. Ge, X. Gao, Y. Li, X. Zhong, L. Wang, H. Lei, X. Zhou, Z. Zhang, L. Cheng, PtCu nanosonosensitizers with inflammatory microenvironment regulation for enhanced sonodynamic bacterial elimination and tissue repair, Adv. Funct. Mater. (2023), 2212489, https://doi.org/10.1002/adfm.202212489.
[99] Y.Z. Zhu, W.L. Hong, X.M. Liu, L. Tan, J. Wu, C.Y. Mao, Y.M. Xiang, S.L. Wu, K.M. C. Cheung, K.W.K. Yeung, Rapid bacterial elimination achieved by sonodynamic Au@Cu2O hybrid nanocubes, Nanoscale 13 (2021) 15699–15710, https://doi.org/10.1039/d1nr04512a.
[100] N. Tao, Z.L. Zeng, Y.Y. Deng, L.M. Chen, J.H. Li, L. Deng, Y.N. Liu, Stanene nanosheets-based hydrogel for sonodynamic treatment of drug-resistant bacterial infection, Chem. Eng. J. 456 (2023), 141109, https://doi.org/10.1016/j.cej.2022.141109.
[101] Y.L. Zheng, W. Wang, Y. Gao, W.Y. Wang, R.W. Zhang, D.J. Wu, L.D. Yu, Y. Chen, Nanosonosensitizers-engineered injectable thermogel for augmented chemo-sonodynamic therapy of melanoma and infected wound healing, Mater. Today Bio 20 (2023) 13, https://doi.org/10.1016/j.mtbio.2023.100621.
[102] M.F. Shen, J.W. Zhou, M. Elhadidy, Y.L. Xianyu, J.S. Feng, D.H. Liu, T. Ding, Cyclodextrin metal-organic framework by ultrasound-assisted rapid synthesis for caffeic acid loading and antibacterial application, Ultrason. Sonochem. 86 (2022) 10, https://doi.org/10.1016/j.ultsonch.2022.106003.
[103] M. Yang, J. Zhang, Y.H. Wei, J. Zhang, C.M. Tao, Recent advances in metal-organic framework-based materials for anti-staphylococcus aureus infection, Nano Res. 15 (2022) 6220–6242, https://doi.org/10.1007/s12274-022-4302-x.
[104] W.M. Yu, W.Q. Zhen, Q.Z. Zhang, Y.C. Li, H.Y. Luo, J. He, Y.M. Liu, Porphyrin-based metal-organic framework compounds as promising nanomedicines in photodynamic therapy, ChemMedChem 15 (2020) 1766–1775, https://doi.org/10.1002/cmdc.202000353.
[105] Y.X. Zeng, Q.L. Ouyang, Y. Yu, L. Tan, X.M. Liu, Y.F. Zheng, S.L. Wu, Defective homojunction porphyrin-based metal-organic frameworks for highly efficient sonodynamic therapy, Small Methods, 7 2201248. 10.1002/smtd.202201248.
[106] X.D. Meng, S.R. Sun, C.C. Gong, J.Y. Yang, Z. Yang, X.J. Zhang, H.F. Dong, Ag-doped metal-organic frameworks' heterostructure for sonodynamic therapy of deep-seated cancer and bacterial infection, ACS Nano, 17 1174-1186. 10.1021/acsnano.2c08687.
[107] Q.Y. Zheng, X.M. Liu, S. Gao, Z.D. Cui, S.L. Wu, Y.Q. Liang, Z.Y. Li, Y.F. Zheng, S. L. Zhu, H. Jiang, R.Q. Zou, Engineering dynamic defect of Ce-III/Ce-IV-based metal-organic framework through ultrasound-triggered Au electron trapper for sonodynamic therapy of osteomyelitis, Small (2023), 2207687, https://doi.org/10.1002/smll.202207687.
[108] W. Guo, Y.M. Wang, K. Zhang, X.G. Dai, Z.Z. Qiao, Z.W. Liu, B.R. Yu, N.A. Zhao, F.J. Xu, Near-infrared light-propelled MOF@Au nanomotors for enhanced penetration and sonodynamic therapy of bacterial biofilms, Chem. Mater. (2023) 12, https://doi.org/10.1021/acs.chemmater.3c01140.
[109] L. Ma, X.G. Zhang, H.C. Wang, X.B. Feng, J. Lei, Y.Q. He, J.Y. Wei, Y.K. Zhang, L. Tan, C. Yang, Two-dimensional Nb2C-based nanoplatform augmented sonodynamic antibacterial therapy and bone regeneration, Sci. China-Mater. 66 (2023) 2913–2924, https://doi.org/10.1007/s40843-022-2413-4.
[110] X.B. Feng, L. Ma, J. Lei, Q.L. Ouyang, Y.X. Zeng, Y. Luo, X.G. Zhang, Y. Song, G. C. Li, L. Tan, X.M. Liu, C. Yang, Piezo-Augmented Sonosensitizer with Strong Ultrasound-Propelling Ability for Efficient Treatment of Osteomyelitis, ACS Nano 16 (2022) 2546–2557, https://doi.org/10.1021/acsnano.1c09189.
[111] Y. Yu, L. Tan, Z.Y. Li, X.M. Liu, Y.F. Zheng, X.B. Feng, Y.Q. Liang, Z.D. Cui, S. L. Zhu, S.L. Wu, Single-atom catalysis for efficient sonodynamic therapy of methicillin-resistant Staphylococcus aureus-infected osteomyelitis, ACS Nano 15 (2021) 10628–10639, https://doi.org/10.1021/acsnano.1c03424.
[112] Y.J. Xin, Z.Y. Guo, A.J. Ma, E.Y. Shi, Z.Y. Li, Z.H. Liang, Z.Y. Qian, L. Yang, Y. S. Wang, M.X. Cao, X.Y. Yang, A robust ROS generation nanoplatform combating periodontitis via sonodynamic/chemodynamic combination therapy, Chem. Eng. J. 451 (2023), 138782, https://doi.org/10.1016/j.cej.2022.138782.
[113] Y.J. Cheng, Y.F. Zhang, Z. Zhao, G. Li, J. Li, A.R. Li, Y. Xue, B.L. Zhu, Z.M. Wu, X. G. Zhang, Guanidinium-decorated nanostructure for precision sonodynamic-catalytic therapy of MRSA-infected osteomyelitis, Adv. Mater. 34 (2022), 2208681, https://doi.org/10.1002/adma.202206646.
[114] G. Shu, Y. Lin, R. Zhong, X. Su, S. Guo, C. Wang, C. Zhou, L. Song, L. Xie, K. Ma, H. Yue, Engineering triple internal electric fields in Ag NWs@BaTiO3 composites for ultrasonic-visible-light driven antibacterial activity, Chem. Eng. J. 463 (2023), 142310, https://doi.org/10.1016/j.cej.2023.142310.
[115] C. Wang, W. Sun, Y. Xiang, S. Wu, Y. Zheng, Y. Zhang, J. Shen, L. Yang, C. Liang, X. Liu, Ultrasound-activated piezoelectric MoS2 enhances sonodynamic for bacterial killing, Small Sci. (2023) 2300022, https://doi.org/10.1002/smsc.202300022.
[116] K.L. Yang, H. Dong, W.J. Xiu, L.H. Yuwen, Y.B. Mou, Z.W. Yin, B. Liang, L. H. Wang, Self-adaptive antibiofilm effect and immune regulation by hollow Cu2MoS4 nanospheres for treatment of implant infections, ACS Appl. Mater. Interfaces 15 (2023) 18720–18733, https://doi.org/10.1021/acsami.3c01928.
[117] H. Wang, N. Mu, Y. He, X. Zhang, J. Lei, C. Yang, L. Ma, Y. Gao, Ultrasound-controlled MXene-based Schottky heterojunction improves anti-infection and osteogenesis properties, Theranostics 13 (2023) 1669–1683, https://doi.org/10.7150/thno.81511.
[118] J. Yu, Z. Guo, J. Yan, C. Bu, C. Peng, C. Li, R. Mao, J. Zhang, Z. Wang, S. Chen, M. Yao, Z. Xie, C. Yang, Y.Y. Yang, P. Yuan, X. Ding, Gastric acid-responsive ROS nanogenerators for effective treatment of Helicobacter pylori infection without disrupting homeostasis of intestinal flora, Adv. Sci. (2023), 2206957, https://doi.org/10.1002/advs.202206957.
[119] D. Simoes, S.P. Miguel, M.P. Ribeiro, P. Coutinho, A.G. Mendonca, I.J. Correia, Recent advances on antimicrobial wound dressing: a review, Eur. J. Pharm. Biopharm. 127 (2018) 130–141, https://doi.org/10.1016/j.ejpb.2018.02.022.
[120] P.Y. Xu, C.P. Fu, R.K. Kankala, S.B. Wang, A.Z. Chen, Supercritical carbon dioxide-assisted nanonization of dihydromyricetin for anticancer and bacterial biofilm inhibition efficacies, J. Supercrit. Fluids 161 (2020), 104840, https://doi.org/10.1016/j.supflu.2020.104840.
[121] A.B.G. Lansdown, U. Mirastschijski, N. Stubbs, E. Scanlon, M.S. Agren, Zinc in wound healing: Theoretical, experimental, and clinical aspects, Wound Repair Regen. 15 (2007) 2–16, https://doi.org/10.1111/j.1524-475X.2006.00179.x.
[122] Y. Xiang, J. Lu, C. Mao, Y. Zhu, C. Wang, J. Wu, X. Liu, S. Wu, K.Y.H. Kwan, K.M. C. Cheung, K.W.K. Yeung, Ultrasound-triggered interfacial engineering-based microneedle for bacterial infection acne treatment, Sci. Adv. 9 (2023), eadf0854, https://doi.org/10.1126/sciadv.adf0854.
[123] D. Huang, Y. Cheng, G. Chen, Y. Zhao, 3D-printed janus piezoelectric patches for sonodynamic bacteria elimination and wound healing, Research 6 (2023) 0022, https://doi.org/10.34133/research.0022.
[124] A. Maleki, J.H. He, S. Bochani, V. Nosrati, M.A. Shahbazi, B.L. Guo, Multifunctional photoactive hydrogels for wound healing acceleration, ACS Nano 15 (2021) 18895–18930, https://doi.org/10.1021/acsnano.1c08334.
[125] D.P. Lew, F.A. Waldvogel, Osteomyelitis, Lancet 364 (2004) 369–379, https://doi.org/10.1016/s0140-6736(04)16727-5.
[126] X. Wang, M. Zhang, T. Zhu, Q. Wei, G. Liu, J. Ding, Flourishing antibacterial strategies for osteomyelitis therapy, Adv. Sci. 10 (2023), 2206154, https://doi.org/10.1002/advs.202206154.
[127] S. Baker, N. Thomson, F.X. Weill, K.E. Holt, Genomic insights into the emergence and spread of antimicrobial-resistant bacterial pathogens, Science 360 (2018) 733–738, https://doi.org/10.1126/science.aar3777.
[128] B. Spellberg, B.A. Lipsky, Systemic antibiotic therapy for chronic osteomyelitis in adults, Clin. Infect. Dis. 54 (2012) 393–407, https://doi.org/10.1093/cid/cir842.
[129] X.W. Wang, X.Y. Zhong, F. Gong, Y. Chao, L. Cheng, Newly developed strategies for improving sonodynamic therapy, Mater. Horizons 7 (2020) 2028–2046, https://doi.org/10.1039/d0mh00613k.
[130] A. Maleki, M. Seyedhamzeh, M. Yuan, T. Agarwal, I. Sharifi, A. Mohammadi, P. Kelicen-Ugur, M. Hamidi, M. Malaki, A.A. Al Kheraif, Z. Cheng, J. Lin, Titanium-based nanoarchitectures for sonodynamic therapy-involved multimodal treatments, Small 19 (2023), 2206253, https://doi.org/10.1002/smll.202206253.
[131] M.R. Rasouli, C. Restrepo, M.G. Maltenfort, J.J. Purtill, J. Parvizi, Risk factors for surgical site infection following total joint arthroplasty, J. Bone Joint Surg.-Am. 96A (2014) e158, https://doi.org/10.2106/jbjs.M.01363.
[132] B.H. Kapadia, S. Banerjee, J.J. Cherian, K.J. Bozic, M.A. Mont, The economic impact of periprosthetic infections after total hip arthroplasty at a specialized tertiary-care center, J. Arthroplast. 31 (2016) 1422–1426, https://doi.org/10.1016/j.arth.2016.01.021.
[133] F. Li, Q.Y. Pan, Y. Ling, J.Y. Guo, Y.R. Huo, C. Xu, M.W. Xiong, M. Yuan, Z. Y. Cheng, M. Liu, J. Lin, Gold-titanium dioxide heterojunction for enhanced sonodynamic mediated biofilm eradication and peri-implant infection treatment, Chem. Eng. J. 460 (2023), 141791, https://doi.org/10.1016/j.cej.2023.141791.

[134] W. Guan, L. Tan, X.M. Liu, Z.D. Cui, Y.F. Zheng, K.W.K. Yeung, D. Zheng, Y. Q. Liang, Z.Y. Li, S.L. Zhu, X.B. Wang, S.L. Wu, Ultrasonic interfacial engineering of red phosphorous-metal for eradicating MRSA infection effectively, Adv. Mater. 33 (2021) 2006047, https://doi.org/10.1002/adma.202006047.
[135] J. Zeng, C. Gu, X. Geng, K. Lin, Y. Xie, X. Chen, Combined photothermal and sonodynamic therapy using a 2D black phosphorus nanosheets loaded coating for efficient bacterial inhibition and bone-implant integration, Biomaterials 297 (2023), 122122, https://doi.org/10.1016/j.biomaterials.2023.122122.
[136] G. Narayanappa, B.N. Nandeesh, Infective myositis, Brain Pathol. 31 (2021) e12950, https://doi.org/10.1111/bpa.12950.
[137] M.L. Song, Y. Cheng, Y. Tian, C.C. Chu, C. Zhang, Z.X. Lu, X.Y. Chen, X. Pang, G. Liu, Sonoactivated chemodynamic therapy: A robust ROS generation nanotheranostic eradicates multidrug-resistant bacterial infection, Adv. Funct. Mater. 30 (2020), 2003587, https://doi.org/10.1002/adfm.202003587.
[138] C.H. Stuart, S.A. Schwartz, T.J. Beeson, C.B. Owatz, Enterococcus faecalis: Its role in root canal treatment failure and current concepts in retreatment, J. Endod. 32 (2006) 93–98, https://doi.org/10.1016/j.joen.2005.10.049.
[139] B. Gomes, J.D. Lilley, D.B. Drucker, Clinical significance of dental root canal microflora, J. Dent. 24 (1996) 47–55, https://doi.org/10.1016/0300-5712(95)00042-9.
[140] R. Park, M. Choi, J. Seo, E.H. Park, S.W. Jang, W.J. Shon, H.Y. Kim, W. Kim, Root canal irrigation system using remotely generated high-power ultrasound, Ultrason. Sonochem. 90 (2022), 106168, https://doi.org/10.1016/j.ultsonch.2022.106168.
[141] J. Dang, M.Q. Zhu, F.H. Dong, R.Q. Zhong, Z.X. Liu, J. Fang, J. Zhang, J. Pan, Ultrasound-activated nanodroplet disruption of the Enterococcus faecalis biofilm in dental root canal, ACS Appl. Bio Mater. 5 (2022) 2135–2142, https://doi.org/10.1021/acsabm.1c01031.
[142] Y. Wang, H.N. Liu, Z. Zhen, K.H. Yiu, H.F. Tse, G. Pelekos, M. Tonetti, L.J. Jin, Periodontal treatment modulates gene expression of endothelial progenitor cells in diabetic patients, J. Clin. Periodontol. 44 (2017) 1253–1263, https://doi.org/10.1111/jcpe.12806.
[143] H. Hasturk, A. Kantarci, Activation and resolution of periodontal inflammation and its systemic impact, Periodontol. 2000 (69) (2015) 255–273, https://doi.org/10.1111/prd.12105.
[144] D.M. Musher, M.S. Abers, J.G. Bartlett, Evolving understanding of the causes of pneumonia in adults, With special attention to the role of pneumococcus, Clin. Infect. Dis. 65 (2017) 1736–1744, https://doi.org/10.1093/cid/cix549.
[145] S. Mitragotri, Innovation - Healing sound: the use of ultrasound in drug delivery and other therapeutic applications, Nat. Rev. Drug Discov. 4 (2005) 255–260, https://doi.org/10.1038/nrd1662.
[146] H. Yu, X. Zhao, Y. Zu, X. Zhang, B. Zu, X. Zhang, Preparation and Characterization of Micronized Artemisinin via a Rapid Expansion of Supercritical Solutions (RESS) Method, Int. J. Mol. Sci. 13 (2012) 5060–5073, https://doi.org/10.3390/ijms13045060.
[147] J. Weers, Inhaled antimicrobial therapy - Barriers to effective treatment, Adv. Drug Deliv. Rev. 85 (2015) 24–43, https://doi.org/10.1016/j.addr.2014.08.013.
[148] X.T. Pan, N. Wu, S.Y. Tian, J. Guo, C.H. Wang, Y. Sun, Z.Z. Huang, F.Z. Chen, Q. Y. Wu, Y. Jing, Z. Yin, B.H. Zhao, X.L. Xiong, H.Y. Liu, D.S. Zhou, Inhalable MOF-derived nanoparticles for sonodynamic therapy of bacterial pneumonia, Adv. Funct. Mater. 32 (2022), 2112145, https://doi.org/10.1002/adfm.202112145.
[149] Y.K. Lai, W. Wei, Y.Q. Du, J. Gao, Z.S. Li, Biomaterials for Helicobacter pylori therapy: therapeutic potential and future perspectives, Gut Microbes 14 (2022), 2120747, https://doi.org/10.1080/19490976.2022.2120747.